Electronic Supplementary Information (ESI)

Type I photosensitizers based on phosphindole oxide for photodynamic therapy: apoptosis and autophagy induced by endoplasmic reticulum stress

Zeyan Zhuang,[a] Jun Dai,[b] Maoxing Yu,[a] Jianqing Li,[a] Pingchuan Shen,[a] Rong Hu,[a] Xiaoding Lou,[c] Zujin Zhao*[a] and Ben Zhong Tang[a,d]

[a] State Key Laboratory of Luminescent Materials and Devices, Guangdong Provincial Key Laboratory of Luminescence from Molecular Aggregates, South China University of Technology, Guangzhou 510640, China.

[b] Department of Obstetrics and Gynecology, Tongji Hospital, Tongji Medical College, Huazhong University of Science and Technology, Wuhan 430074, China.

[c] Engineering Research Center of Nano-Geomaterials of Ministry of Education, Faculty of Materials Science and Chemistry, China University of Geosciences, Wuhan 430074, China.

[d] Department of Chemistry, The Hong Kong University of Science & Technology, Clear Water Bay, Kowloon, Hong Kong, China.

*Correspondence: mszjzhao@scut.edu.cn

Contents

1. General information and methods

1.1 Materials

Tetrahydrofuran (THF) was distilled from sodium benzophenone ketyl under dry nitrogen immediately prior to use. Ultrapure water was supplied by Milli-Q Plus System (Millipore Corporation, United States). Compound **3** was prepared according to the reported literature.[1] Phosphate buffered saline (PBS), fetal bovine serum (FBS), penicillin, streptomycin, were purchased from Thermo Fisher Scientific. Dulbecco's Modified Essential Medium (DMEM) was purchased from Gibco (Life Technologies). 3-(4,5-Dimethyl-2-thiazolyl)-2,5-diphenyl-2H-tetrazolium bromide (MTT) was purchased from J&K Scientific Ltd. The HeLa cell lines were purchased from the Cell Resource Center, Peking Union Medical College. The SKOV-3 cell lines were purchased from Boshide Biological Technology Co., Ltd. The female BALB/c nude mice (5-week-old) were purchased from Beijing Vital River Laboratory Animal Technology Co., Ltd. Other chemicals and reagents were purchased from commercial sources and used as received without further purification.

1.2 Instruments

^{1}H and ^{13}C NMR spectra were measured on a Bruker AV 500 spectrometer in deuterated dichloromethane using tetramethylsilane (TMS; $\delta = 0$) as internal reference at room temperature. High resolution mass spectra (HRMS) were recorded on a GCT premier CAB048 mass spectrometer operating in a MALDT-TOF mode. UV-vis absorption spectra were measured on a SHIMADZU UV-2600 spectrophotometer. Photoluminescence spectra were recorded on a Horiba Fluoromax-4 fluorescence spectrophotometer. Fluorescence quantum yields were measured using a Hamamatsu absolute PL quantum yield spectrometer C11347 Quantaurus_QY. Particle size analysis was performed on a Malvern Zetasizer Nano-S90. Cyclic voltammetry was measured on a CHI 630E electrochemical analyzer. The Electron paramagnetic resonance (EPR) measurements were carried out on Bruker ELEXSYS-II E500 in X-band. Confocal laser scanning microscopy (CLSM) images were obtained on a Zeiss LSM7 DUO Laser Scanning Confocal Microscope. Automated cell counter (Countess II) was employed for cell counting. The cell viability analysis for estimating cytotoxicity was collected using a microplate reader (Tecan Infinite M200PRO) at a wavelength of 570 nm. The white light source was a CXE-350 xenon lamp fiber illumination system produced by Photoelectronic Instrument Factory of Beijing Normal University. The irradiation light energy

density was measured using an FZ-A irradiatometer produced by Photoelectronic Instrument Factory of Beijing Normal University. Bio-rad Mini-PROTEAN® system was employed for electrophoresis and membrane transfer. The *in vitro* hypoxic condition[2] was created using microaerophilic AnaeroPack produced by Mtsubishi Gas Chemical Company, Inc. Western blotting documentation was performed on an X-ray camera cassette produced by Yijia Biotechnology, using Fuji X-ray film. Imaging of mouse was performed by using IVIS Spectrum imaging system from Perkin Elmer. The ground-state and excited-state geometries in THF were optimized using the density function theory (DFT) and time-dependent density function theory (TD-DFT) method, respectively, with M06-2X hybrid functional at the basis set level of 6-311G (d,p) under the solvent model of Solvation Model Based on Density (SMD), performed using Gaussian 09 package, Revision D.01.[3] No symmetry constraint was applied for optimization. The electron and hole analysis and atomic dipole moment corrected Hirshfeld (ADCH) analysis were performed with Multiwfn 3.6. The spin-orbit coupling (SOC) values were calculated by using Dalton, Release v2016.2.[4]

2. Methods and Experimental Procedure

2.1 Cyclic voltammetry measurement

The cyclic voltammetry measurement was conducted in dichloromethane (for positive scan) or *N*,*N*-dimethylformamide (DMF, for negative scan) with 0.1 M tetrabutylammonium hexafluorophosphate as the supporting electrolyte at a scan rate of 100 mV s^{-1} using platinum as the working electrode, saturated calomel electrode (SCE) as the reference electrode and platinum wire counter electrode. The SCE reference electrode was calibrated using the ferrocene/ferrocenium (Fc/Fc^{+}) redox couple as an external standard.

2.2 ROS generation measurement in aqueous media

2.2.1 General ROS detection by fluorescence analysis

The general ROS generation measurements were conducted using 2,7-dichlorodihydrofluorescein (DCFH) as the indicator, which was converted from 2,7-dichlorodihydrofluorescein diacetate (DCFH-DA, 0.5 mL, 1 mM in ethanol) reacting with aqueous solution of NaOH (2 mL, 1.0 mM) for 30 min at room temperature. The hydrolysate was then neutralized with 7.5 mL PBS buffer solution to get the stock solution with a concentration of 50 μM. PBS buffer solution containing 1 μM DCFH was added 1 μM *α*-TPA-PIO (stock solution: 0.1 mM in dimethylsulfoxide (DMSO)), *β*-TPA-PIO

(stock solution: 0.1 mM in DMSO), crystal violet (CV, stock solution: 0.1 mM in water with additional DMSO), methylene blue (MB, stock solution: 0.1 mM in water with additional DMSO), or pure DMSO. Additional 500 nM/5 μM bovine serum albumin (BSA, stock solution: 0.1 mM in water) was added in the substrate-containing group. The fluorescence signal of indicator was monitored in a range of 510–560 nm with the excitation wavelength at 504 nm after the solution was irradiated by white light irradiation of 20 mW cm^{-2}. The fluorescence intensity change at 522 nm was recorded to indicate the ROS generation rate.

2.2.2 $OH^{\bullet}$ detection by fluorescence analysis

The $OH^{\bullet}$ generation measurements were conducted using hydroxyphenyl fluorescein (HPF) as the indicator. PBS buffer solution containing 5 μM HPF (stock solution: 5 mM in DMF) was added 1 μM *α*-TPA-PIO (stock solution: 0.1 mM in DMSO), *β*-TPA-PIO (stock solution: 0.1 mM in DMSO), CV (stock solution: 0.1 mM in water with additional DMSO), or pure DMSO. Additional 500 nM/5 μM BSA (stock solution: 0.1 mM in water) was added in the substrate-containing group. The fluorescence signal of indicator was monitored in a range of 500–550 nm with the excitation wavelength at 480 nm after the solution was irradiated by white light irradiation of 20 mW cm^{-2}. The fluorescence intensity at 514 nm was recorded to indicate the $OH^{\bullet}$ generation rate.

2.2.3 Type I ROS detection by EPR analysis

EPR analysis was performed to monitor the generation of Type I ROS using 5-tert-butoxycarbonyl-5-methyl-1-pyrroline-*N*-oxide (BMPO) as spin-trap agent. PBS buffer solution containing 20 mM BMPO was added 10 μM *α*-TPA-PIO (stock solution: 1 mM in DMSO), *β*-TPA-PIO (stock solution: 1 mM in DMSO), CV (stock solution: 1 mM in water with additional DMSO), or pure DMSO. Additional 5 μM BSA (stock solution: 1 mM in water) was added in the substrate-containing group. Spectra of spin was monitored in a range of 3350–3650 G after the solution was irradiated by irradiation white light of 100 mW cm^{-2} for 5 min. Background interference was corrected using the sample before irradiation.

2.2.4 $^1O_2$ detection by fluorescence analysis

The $^1O_2$ generation measurements were conducted using Singlet Oxygen Sensor Green (SOSG) and 9,10-anthracenediyl-bis(methylene) dimalonic acid (ABDA) as the indicator.

PBS buffer solution containing 5 μM SOSG (stock solution: 5 mM in DMSO) was added 1 μM *α*-TPA-PIO (stock solution: 0.1 mM in DMSO), *β*-TPA-PIO (stock solution: 0.1 mM in DMSO), MB

(stock solution: 0.1 mM in water with additional DMSO), or pure DMSO. The fluorescence signal of indicator was monitored in a range of 510–560 nm with the excitation wavelength at 480 nm after the solution was irradiated by white light irradiation of 20 mW cm^{-2}. The fluorescence intensity at 527 nm was recorded to indicate the $^1O_2$ generation rate.

PBS buffer solution containing 10 μM ABDA (stock solution: 10 mM in DMSO) was added 1 μM *α*-TPA-PIO (stock solution: 0.1 mM in DMSO), *β*-TPA-PIO (stock solution: 0.1 mM in DMSO), MB (stock solution: 0.1 mM in water with additional DMSO), or pure DMSO. The absorption spectra of indicator were monitored in a range of 330–450 nm with the excitation wavelength at 480 nm after the solution was irradiated by white light irradiation of 20 mW cm^{-2}. The absorptance decline relative to the initial value at 380 nm was recorded to indicate the decomposition rates of ABDA ($^1O_2$ generation rate).

2.3 Cellular study

2.3.1 Cell cultures

HeLa cells were cultured in DMEM medium containing 10% FBS and antibiotics (100 units/mL penicillin and 100 μg/mL streptomycin) in a humidified incubator with 5% CO_2 at 37 ^oC.

2.3.2 Biocompatibility measurement

Hela cells were seeded in 96-well plates at a density of 1×10^5 cells/mL. After 24 h of culture, different concentrations of *α*-TPA-PIO or *β*-TPA-PIO were added and incubated at 37 ^oC for 24/36/48 h in dark. The sample and control wells were washed twice with PBS buffer and added with freshly prepared 100 μL MTT solution (0.5 mg/mL). After incubation at 37 ^oC for 4 h, the MTT solution was removed and washed twice with PBS buffer. 100 μL DMSO was then added into each well and the plate was gently shaken for 3 min at room temperature to dissolve all the precipitates formed. The absorbance of sample and control wells at 570 nm was then measured by a microplate Reader. Cell viability was then calculated by the ratio of the absorbance of sample wells to control cells.

2.3.3 Cell imaging

HeLa cells were grown in a confocal imaging dish at 37 ^oC. After incubation with medium containing 1 μM *α*-TPA-PIO or *β*-TPA-PIO (stock solution: 1 mM in DMSO) for 30 min, the cells were imaged by CLSM in the channel mode as well as lambda mode at excitation of 405 nm without further washed. The emission filter was 415−725 nm.

2.3.4 Confocal co-localization

HeLa cells were grown in a confocal imaging dish at 37 °C. HeLa cells were first incubated with 1 mL medium containing commercial dyes ER-Tracker Red (1 μM, stock solution: 1 mM in DMSO), Mito-Tracker Red (100 nM, stock solution: 100 μM in DMSO), Lyso-Tracker Red (100 nM, stock solution: 100 μM in DMSO) or HCS LipidTOX™ Deep Red neutral lipid stain (Art. No.: Invitrogen H34477, 1/1000 dilution),[5] at 37 °C for 30 min. The medium was then removed. After rinsed with PBS for three times and then stained with medium containing 1 μM *α*-TPA-PIO or *β*-TPA-PIO (stock solution: 1 mM in DMSO) for 30 min, the cells were imaged using CLSM. For *α*-TPA-PIO and *β*-TPA-PIO, the excitation was 405 nm and the emission filter was 420–580 nm; For ER-Tracker Red, Mito-Tracker Red and Lyso-Tracker Red, the excitation was 488 nm, and the emission filter was 590–720 nm; For HCS LipidTOX™ Deep Red neutral lipid stain, the excitation was 633 nm, and the emission filter was 640–740 nm.

2.4 ROS generation measurement in vitro

2.4.1 General ROS detection

HeLa cells were grown in a confocal imaging dish at 37 °C. After incubation with medium containing 10 μM *α*-TPA-PIO, *β*-TPA-PIO (stock solution: 1 mM in DMSO) or pure DMSO for 30 min and treatment with medium containing 10 μM DCFH-DA (stock solution: 1 mM in ethanol) for 30 min at 37 °C, the cells were imaged by CLSM at excitation of 488 nm with continuous irradiation of 405 nm laser of 1% power in the designated area. The signal intensity was recorded at every 10 s and measured using ZEN 2012 (blue edition) software. The emission filter was 495–550 nm.

2.4.2 $O_2^{\bullet-}$ detection

HeLa cells were grown in a confocal imaging dish at 37 °C. After incubation with medium containing 10 μM *α*-TPA-PIO, *β*-TPA-PIO (stock solution: 1 mM in DMSO) or pure DMSO for 30 min and treatment with medium containing 5 μM DHE (stock solution: 1 mM in DMSO) for 30 min at 37 °C, the cells were imaged by CLSM at excitation of 488 nm with continuous irradiation of 405 nm laser of 1% power in the designated area. The signal intensity was recorded at every 10 s and measured using ZEN 2012 (blue edition) software. The emission filter was 580–650 nm.

2.4.3 $OH^{\bullet}$ detection

HeLa cells were grown in a confocal imaging dish at 37 °C. After incubation with medium containing 10 μM *α*-TPA-PIO, *β*-TPA-PIO (stock solution: 1 mM in DMSO) or pure DMSO for 30

min and treatment with medium containing 5 μM HPF (stock solution: 1 mM in DMF) for 30 min at 37 °C, the cells were imaged by CLSM at excitation of 488 nm with continuous irradiation of 405 nm laser of 1% power in the designated area. The signal intensity was recorded at every 10 s and measured using ZEN 2012 (blue edition) software. The emission filter was 495−550 nm.

2.5 PDT in vitro

2.5.1 In vitro PDT evaluation

Hela cells were seeded in 96-well plates at a density of 1×10^5 cells/mL. After 24 h of culture, different concentrations of *α*-TPA-PIO or *β*-TPA-PIO were added and incubated at 37 °C for 30 min in dark. Without or with the exposure to white light irradiation of 20 mW cm^{-2} for different time, the cells were further incubated at 37 °C to 24 h. MTT assay was conduced as described in *2.3.2*.

2.5.2 Live/dead cell co-staining assay

HeLa cells were grown in a confocal imaging dish at 37 °C in normal condition or in hypoxic condition. After incubation with medium containing 10 μM *α*-TPA-PIO, *β*-TPA-PIO (stock solution: 1 mM in DMSO) or pure DMSO for 30 min in normal condition or in hypoxic condition. With the exposure to white light irradiation of 20 mW cm^{-2} for 30 min, the cells were further incubated at 37 °C to 24 h in normal condition or in hypoxic condition. Then after stained with medium containing 2 μM calcein-AM (stock solution: 1 mM in DMSO) and 2 μg/mL PI (stock solution: 1 mg/mL in DMSO) for 10 min, the cells were imaged using CLSM. For calcein-AM, the excitation was 488 nm, and the emission filter was 490−540 nm; For PI, the excitation was 543 nm, and the emission filter was 590−680 nm.

2.5.3 Western blot analysis

Protein levels in Hela cells received various treatments were analyzed by Western blot. The cells were lysed using Sodium dodecyl sulfate (SDS) Lysis Buffer containing protease and phosphatase inhibitor. Equal amounts of proteins quantified by BCA Protein Assay Kit were electrophoresed on 12% polyacrylamide gels and transferred to a polyvinylidene fluoride membrane. After blocking with 5% skim milk for 1 h, primary antibody, namely anti-GRP78 (Abcam), anti-CHOP (Affinity), anti-Bcl-2 (Abcam), anti-cleaved caspase-3 (Abcam), anti-LC3B (Abcam) or anti-GAPDH (Yijia Biotechnology), was bound for 1 h. After washing with PBS-Tween, the membrane was incubated with secondary antibody (Yijia Biotechnology) for 1 h at room temperature. Detection was carried out with electrochemiluminescent (ECL) HRP substrate, documented with X-ray film for

visualization. The grayscale image of each labeled protein band was analyzed using ImageJ software.

2.5.4 Cell apoptosis analysis

HeLa cells were grown in a confocal imaging dish at 37 °C. After incubation with medium containing 10 μM *β*-TPA-PIO (stock solution: 1 mM in DMSO) for 30 min for 30 min. With the exposure to white light irradiation of 20 mW cm^{-2} for 30 min, the cells were further incubated at 37 °C to 12 h. The positive control group was treated with medium containing 880 μM H_2O_2 (stock solution: 3% aqueous solution) for 6 h. Then after stained with medium containing annexin V-Alexa Fluor™ 488 conjugate (1/200 dilution) as secondary antobody and 2 μg/mL PI (stock solution: 1 mg/mL in DMSO) for 30 min, the cells were imaged using CLSM. For annexin V-Alexa Fluor™ 488 conjugate, the excitation was 488 nm, and the emission filter was 490–550 nm; For PI, the excitation was 543 nm, and the emission filter was 615–680 nm.

2.5.5 Immunofluorescence images of LC3B

HeLa cells were grown in a confocal imaging dish at 37 °C. After incubation with medium containing 10 μM *β*-TPA-PIO (stock solution: 1 mM in DMSO) or pure DMSO for 30 min. With the exposure to white light irradiation of 20 mW cm^{-2} for 30 min, the cells were further incubated at 37 °C for another 2 h. Then the cells were fixed with 4% paraformaldehyde for 15 min at room temperature, permeabilized with 0.2% Triton X-100 for 15 minutes at room temperature and then blocked with 5% skim milk in 0.2% PBS-T for 1 h. The cells were then incubated overnight at 4 °C with anti-LC3B antibody (Abcam) followed by a further incubation at room temperature for 2 h with an Alexa Fluor® 488 secondary (Beyotime). The cells were then imaged using CLSM. The excitation was 488 nm, and the emission filter was 490–550 nm.

2.6 β-TPA-PIO mediated PDT in vivo

2.6.1 Subcutaneous tumor model

All mice were kept in SPF-level feeding rooms with adequate water and food. The temperature of the feeding room is kept at 26 °C, the humidity is 50% and a 12-hour light/dark cycle. The 5-week-old nude mice were inoculated subcutaneously with SKOV-3 cells (1×10^6 cells) into the right front flanks to establish the liver tumor model. Tumor growth was measured using a caliper, and tumor volume was calculated using the formula: tumor volume = width × width × length/2. When tumors reached an average volume of 50 mm^3, mice were used for *in vivo* imaging and PDT evaluation.

2.6.2 In vivo imaging

β-TPA-PIO (1 mM, 25 μL/50 mm^3 tumor) was injected into the tumors *in situ*. After 24 hours, *in vivo* fluorescence imaging was visualized on IVIS Spectrum imaging system. The excitation was 430 nm, and the collected emission was 580 nm.

2.6.3 In vivo PDT evaluation

All mice were randomly divided into three groups (n = 5): PBS (light +), *β*-TPA-PIO (light –) and *β*-TPA-PIO (light +) groups. *β*-TPA-PIO (1 mM, 25 μL/50 mm^3 tumor) was injected into the tumors *in situ*. After 24 hours, mice in PBS (light +) and *β*-TPA-PIO (light +) groups were irradiated with white light of 200 mW cm^{-2} for 15 minutes, while *β*-TPA-PIO (light –) group was not administered. Body weight and tumor volumes were measured once in 3 days. The mice after 25 days post-PDT were sacrificed and the tumor and the major organs (liver, spleen, kidney, heart and lung) were harvested. The collected tissues were fixed in formalin, which were then processed into paraffin, sliced at thickness of 4 μm for further analysis.

2.6.4 Histological analysis

The slices were stained with hematoxylin and eosin (H&E) and imaged by optical microscopy, according to the manufacturer's instructions.

2.6.5 Terminal deoxynucleotidyl transferase dUTP nickend labeling (TUNEL) assay

Apoptosis in tumor tissues was evaluated by TUNEL assay using a TUNEL Assay Kit. 50 μL of 0.1% Triton X-100 was added on to slides and incubated at room temperature for 10 min. TUNEL (DAPI) substrate was added for nuclear staining. The slides were washed with PBS three times and observed under fluorescence microscope. TUNEL positive signal was collected under excitation of 488 nm in green channel; DAPI signal was collected under excitation of 365 nm in blue channel.

2.6.6 Immunohistochemical (IHC) Staining

The slices were dewaxed in xylene and dehydrated with gradient ethanol. A nonspecific stain blocking agent was added to slides, which were then incubated for 30 min at room temperature. The primary antibody, namely anti-GRP78 (Abcam), anti-CHOP (Affinity), anti-Bcl-2 (Beyotime), anti-cleaved caspase-3 (Cell Signaling Technology), anti-LC3B (Abcam) or anti-Ki-67 (Abcam), was added and slides incubated overnight at 4°C. After washing in PBS three times, the slides were incubated with secondary antibody (Zsbio) for 30 min at room temperature. The complex was visualized with 3,3'-diaminobenzidine complex, and the nuclei were counterstained with haematoxylin. The slices with brown or yellow cytoplasm were considered to be positive.

3. Supplementary Figures and Tables

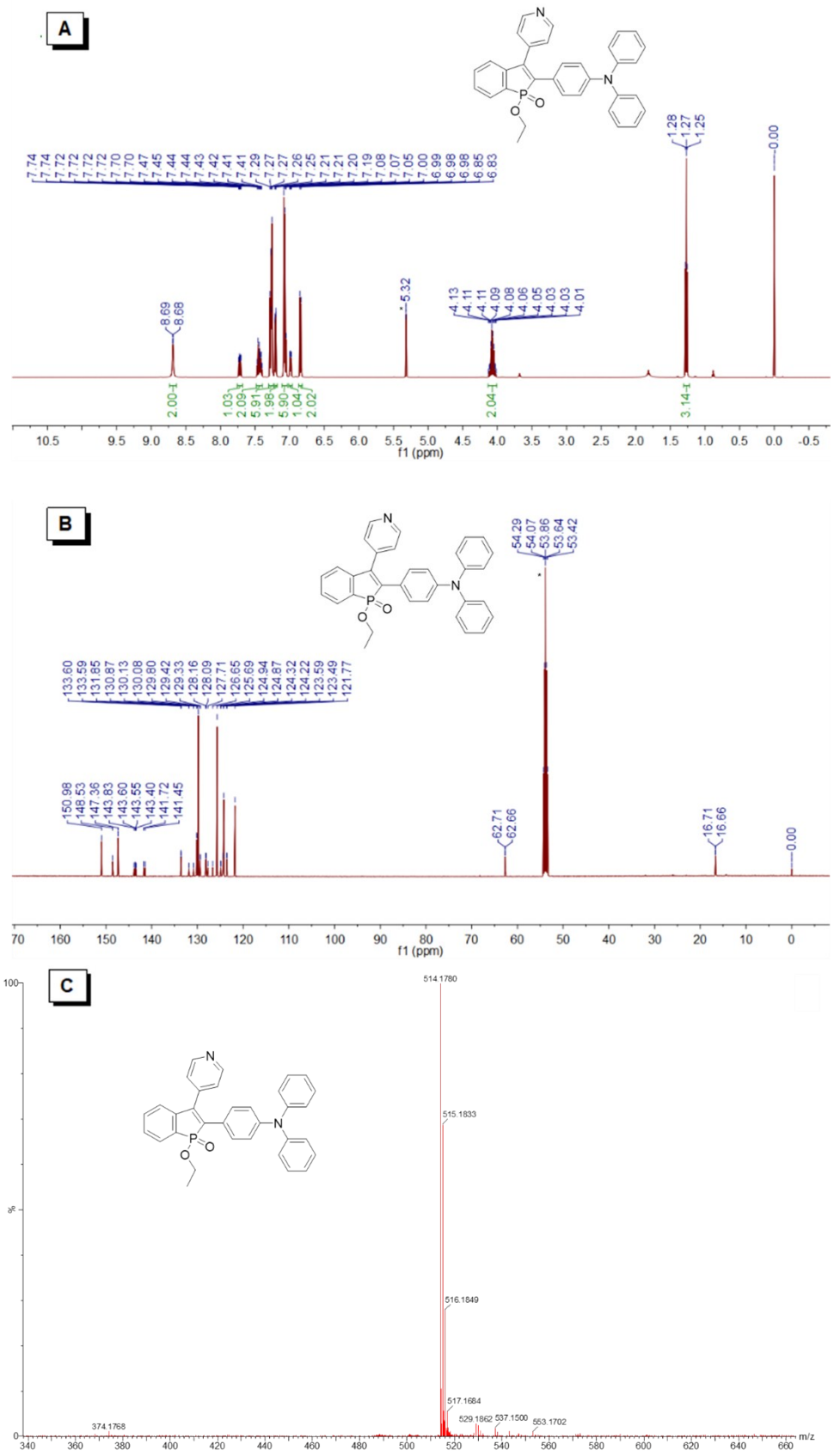

Figure S1. (A) ^{1}H NMR, (B) ^{13}C NMR and (C) HRMS spectra of α-TPA-PIO.

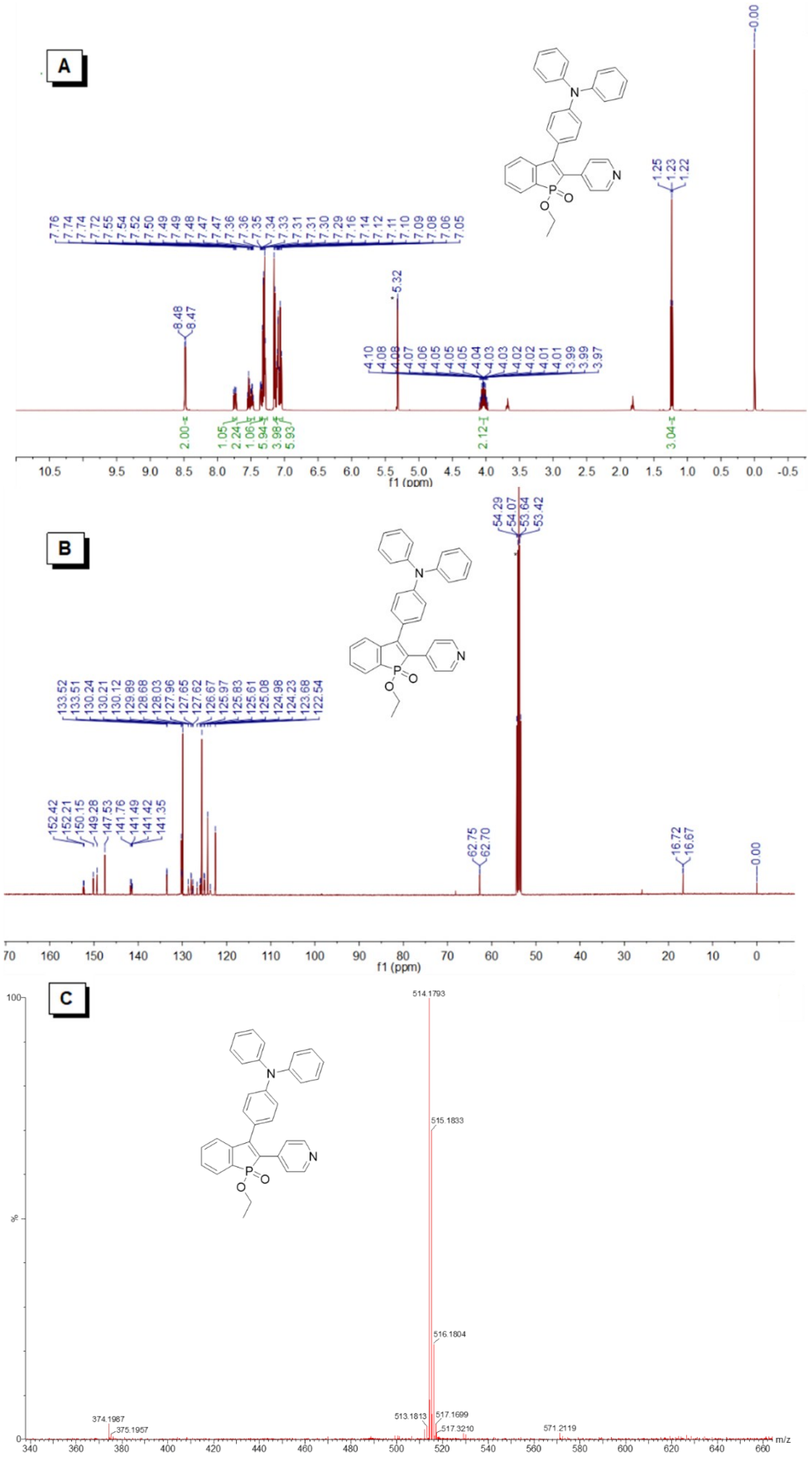

Figure S2. (A) ^{1}H NMR, (B) ^{13}C NMR and (C) HRMS spectra of *β*-TPA-PIO.

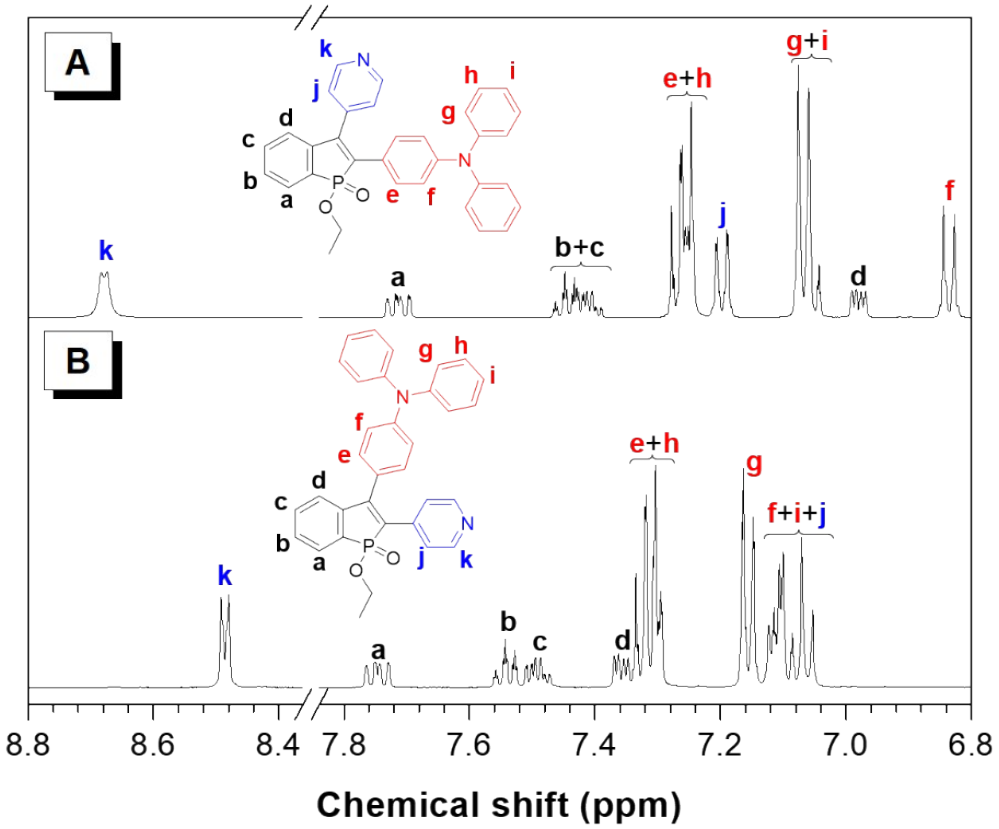

Figure S3. ^{1}H NMR spectra of (A) *α*-TPA-PIO and (B) *β*-TPA-PIO in CD_2Cl_2.

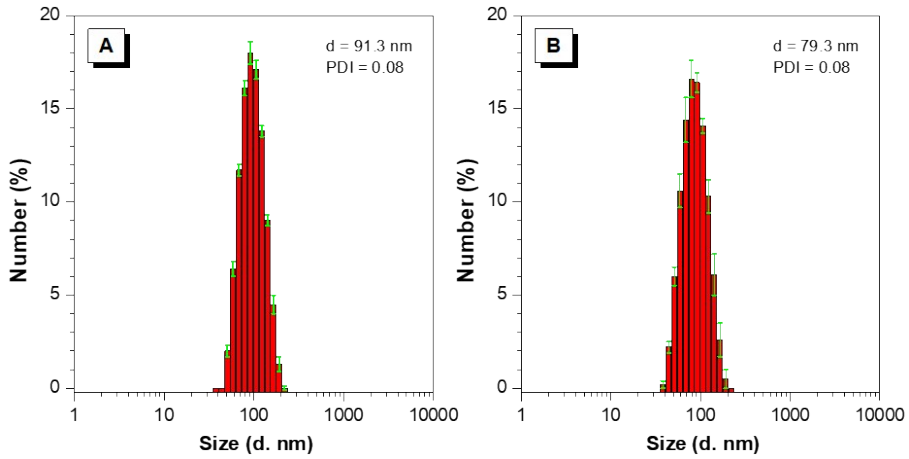

Figure S4. Particle size distribution of (A) *α*-TPA-PIO and (B) *β*-TPA-PIO with average diameter (d) and polydispersity indexes (PDI) measured by dynamic light scattering.

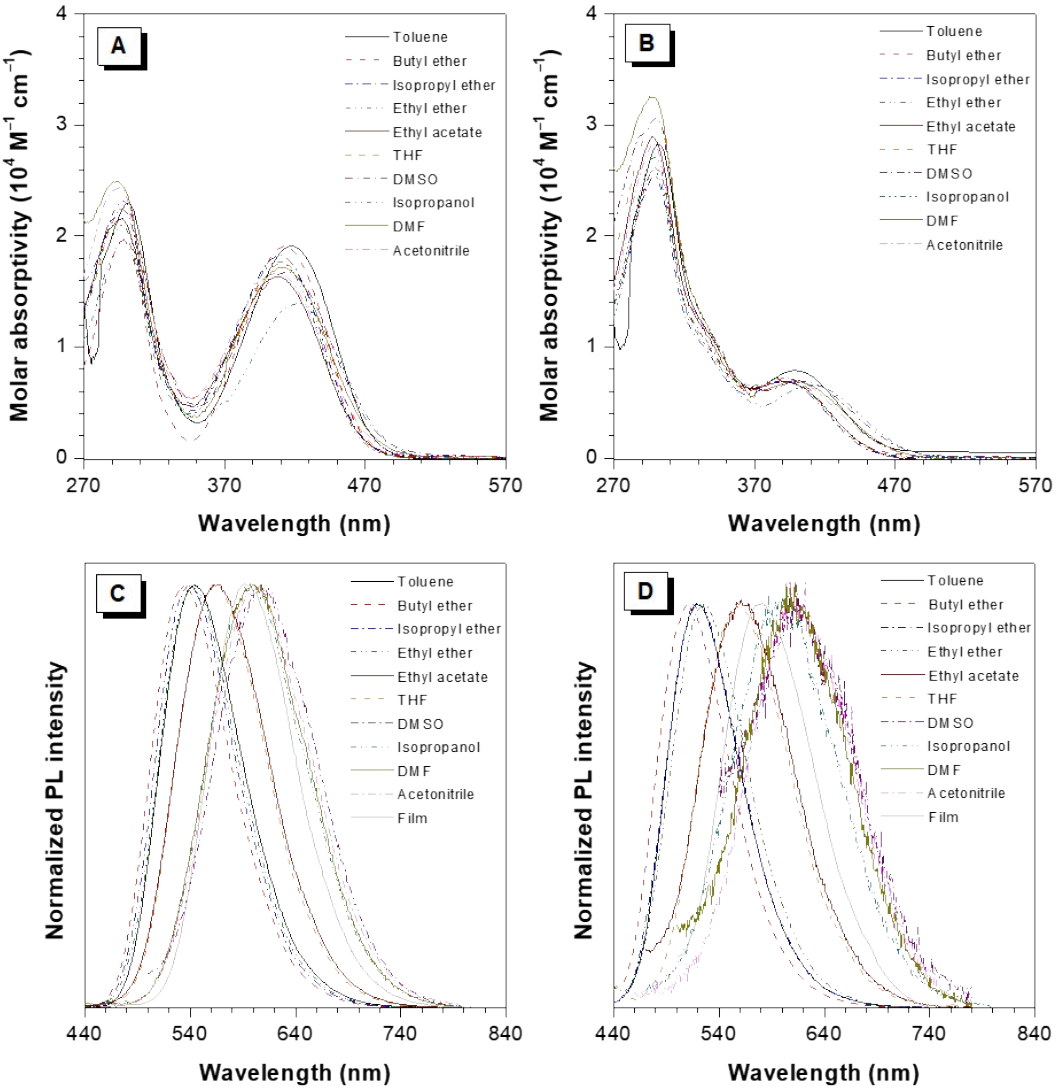

Figure S5. Absorption spectra of (A) *α*-TPA-PIO and (B) *β*-TPA-PIO in various solvents with different polarities (concentration: 10 μM). Normalized PL spectra of (C) *α*-TPA-PIO and (D) *β*-TPA-PIO in various solvents with different polarities (concentration: 10 μM) and in films, excited at the maximum absorption wavelength.

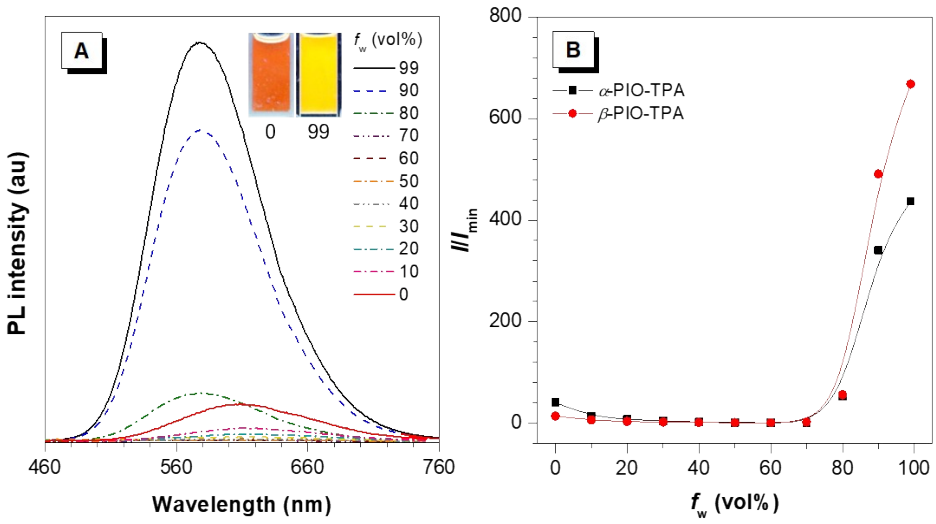

Figure S6. (A) PL spectra of α-TPA-PIO in DMSO/water mixtures with different water fractions (f_ws), excited at 415 nm. Inset: Photos of solutions of α-TPA-PIO in DMSO/water mixtures (f_w = 0 and 99 vol%), taken under the illumination of a UV lamp (365 nm). (B) Plots of I/I_{min} *vs.* f_w for α-TPA-PIO and β-TPA-PIO in DMSO/water mixtures with different f_ws; I_{min} is the PL intensity of the sample with lowest intensity. The PL peak locations are not given because the emissions of several samples are too weak to be measured.

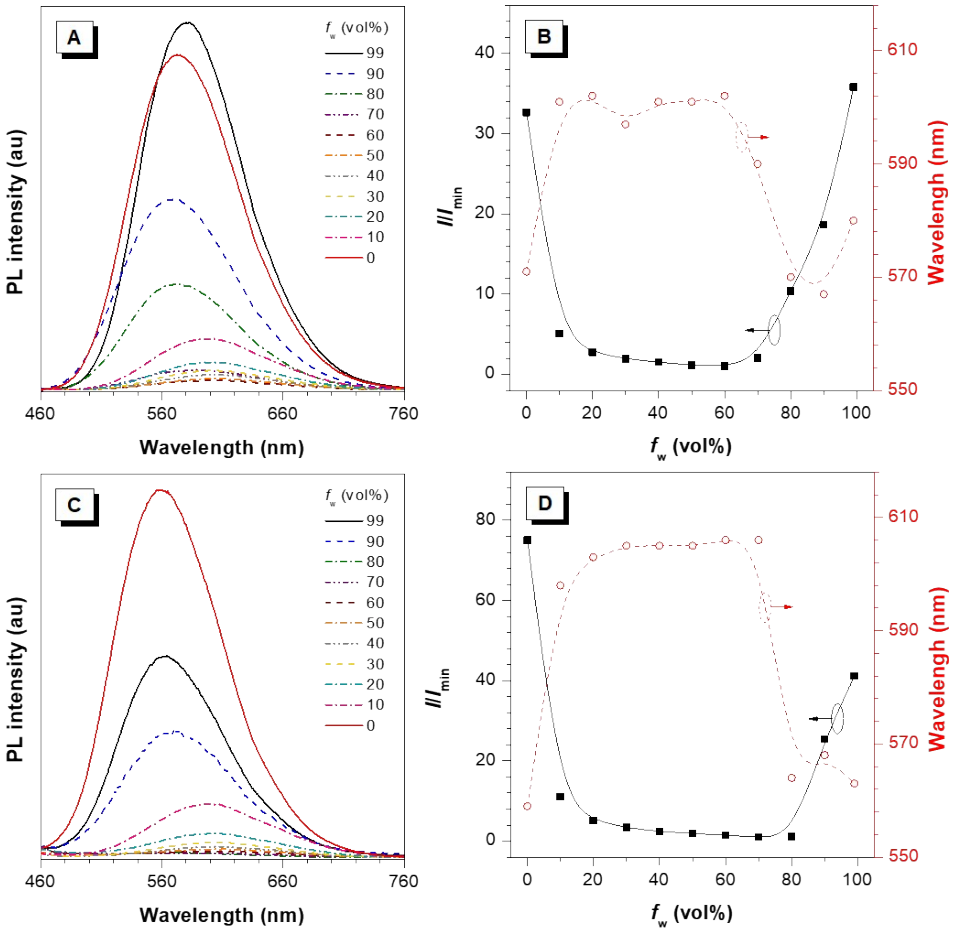

Figure S7. PL spectra of (A) *α*-TPA-PIO and (C) *β*-TPA-PIO in THF/water mixtures with different water fractions (f_ws), excited at 410 nm and 390 nm, respectively. Plots of I/I_{min} and PL peak location *vs.* f_w for (B) *α*-TPA-PIO and (D) *β*-TPA-PIO in THF/water mixtures with different f_ws; I_{min} is the PL intensity of the sample with lowest intensity.

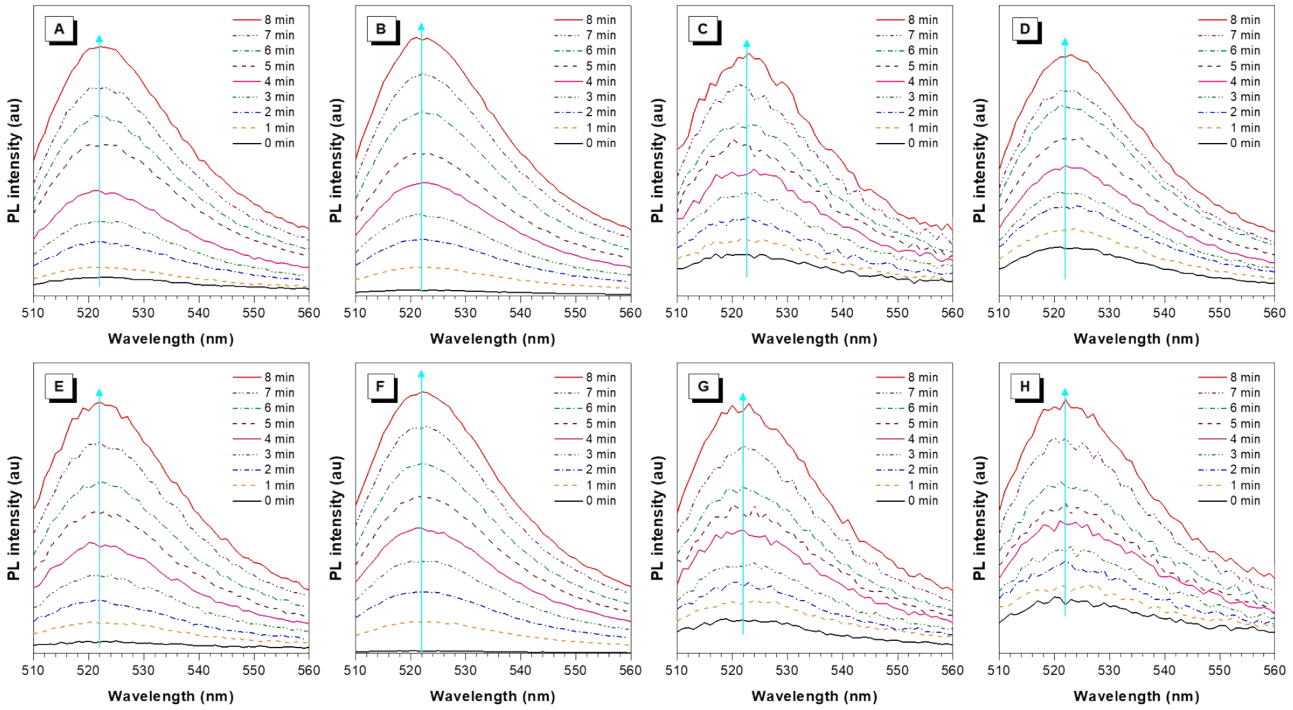

Figure S8. PL spectra of DCFH in PBS in the presence of (A) *α*-TPA-PIO, (B) *β*-TPA-PIO, (C) CV, (D) pure DMSO, (E) *α*-TPA-PIO + BSA, (F) *β*-TPA-PIO + BSA, (G) CV + BSA or (H) BSA after exposure to white light irradiation of 20 mW cm^{-2} with different time. [BSA] = 500 nM.

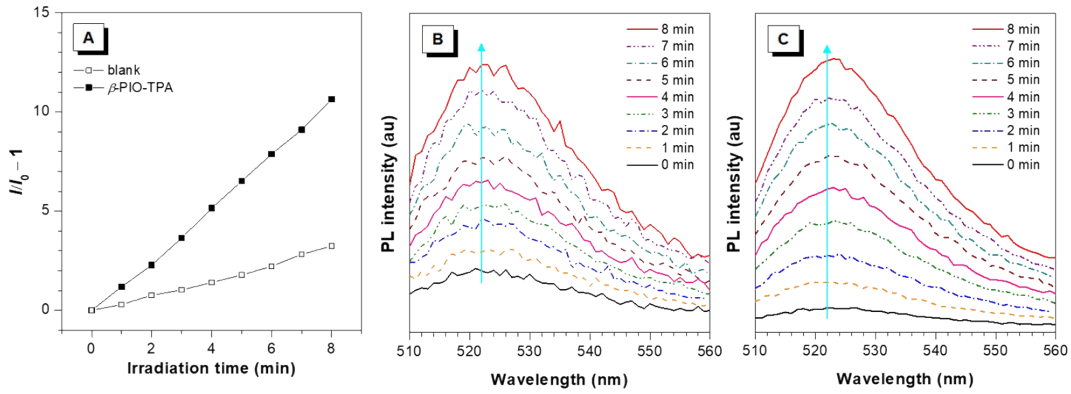

Figure S9. (A) Plots of relative PL intensity of DCFH for general ROS detection in the presence of *β*-TPA-PIO (without/with 5 μM BSA) in PBS with 1% DMSO *vs.* irradiation time (white light, 20 mW cm^{-2}). I_0 and I are the PL intensity of indicator before and after irradiation, respectively. PL spectra of DCFH in PBS in present of (B) BSA or (C) *β*-TPA-PIO + BSA after exposure to white light irradiation of 20 mW cm^{-2} with different time. [BSA] = 5 μM.

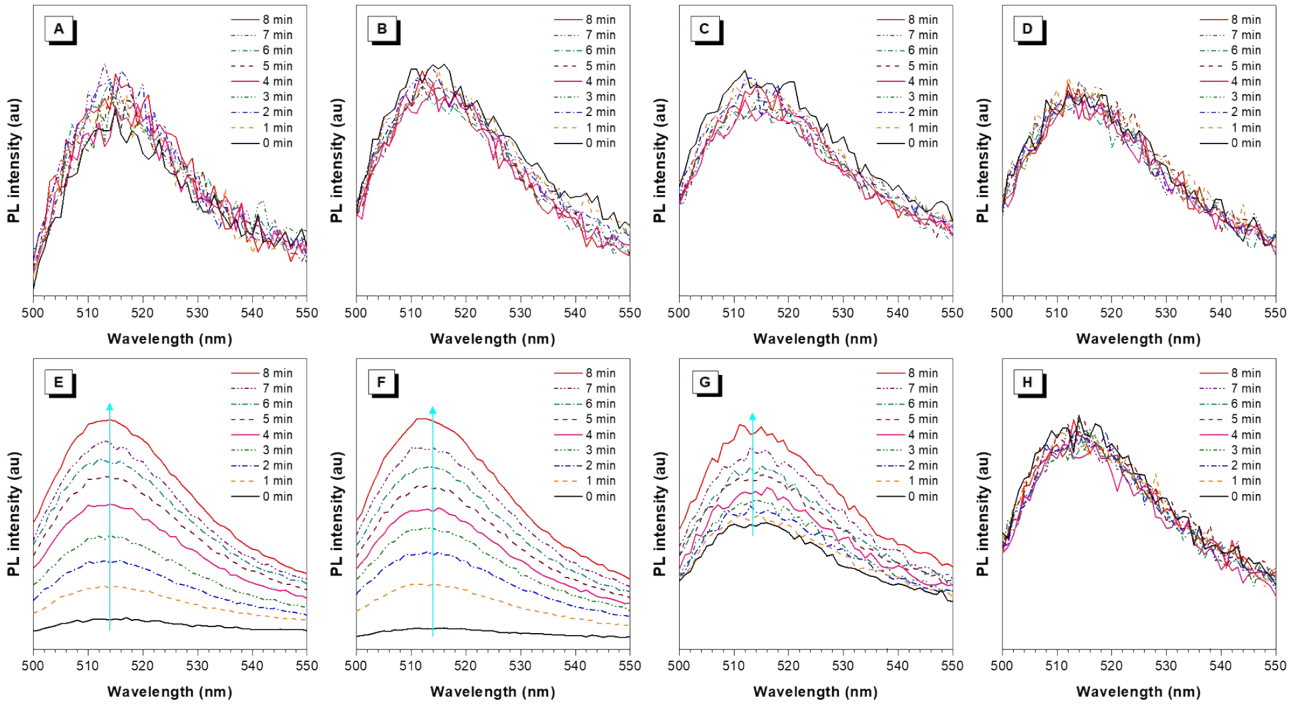

Figure S10. PL spectra of HPF in PBS in the presence of (A) *α*-TPA-PIO, (B) *β*-TPA-PIO, (C) CV, (D) pure DMSO, (E) *α*-TPA-PIO + BSA, (F) *β*-TPA-PIO + BSA, (G) CV + BSA or (H) BSA after exposure to white light irradiation of 20 mW cm^{-2} with different time. [BSA] = 500 nM.

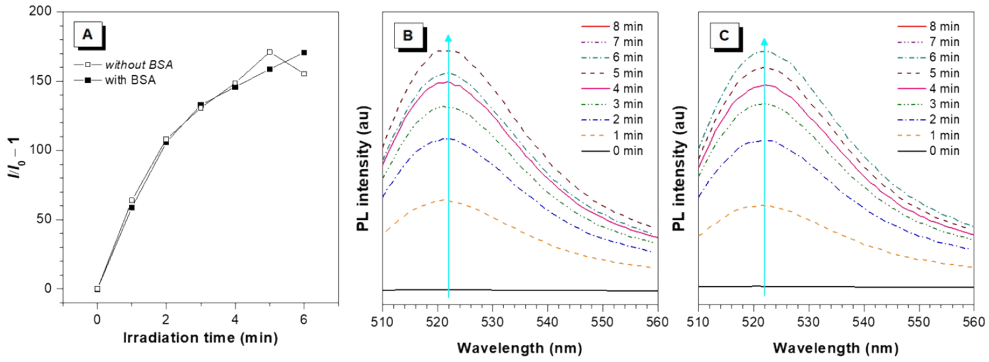

Figure S11. (A) Plots of relative PL intensity of DCFH for general ROS detection in the presence of *β*-TPA-PIO (without/with 500 nM BSA) in PBS with 1% DMSO *vs.* irradiation time (white light, 20 mW cm^{-2}). I_0 and I are the PL intensity of indicator before and after irradiation, respectively. PL spectra of DCFH in PBS in present of (B) BSA or (C) MB + BSA after exposure to white light irradiation of 20 mW cm^{-2} with different time. [BSA] = 500 nM.

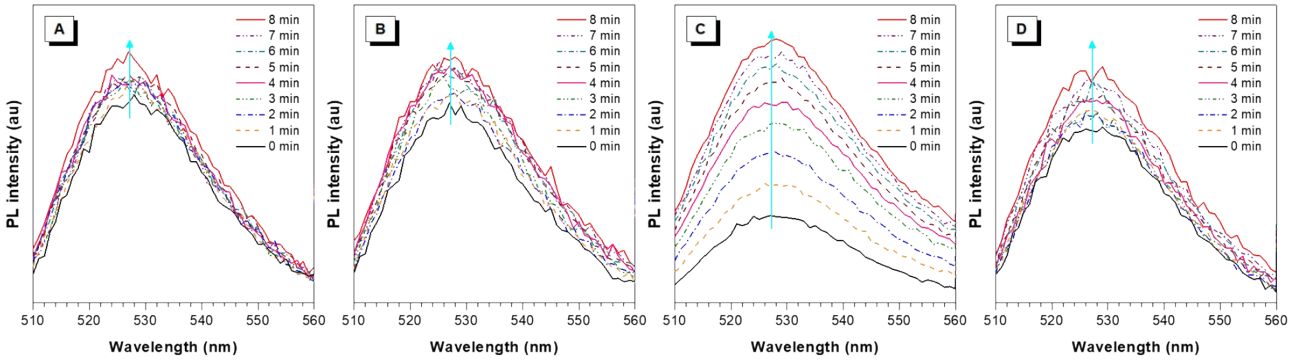

Figure S12. PL spectra of SOSG in PBS in the presence of (A) *α*-TPA-PIO, (B) *β*-TPA-PIO, (C) MB or (D) pure DMSO after exposure to white light irradiation of 20 mW cm^{-2} with different time.

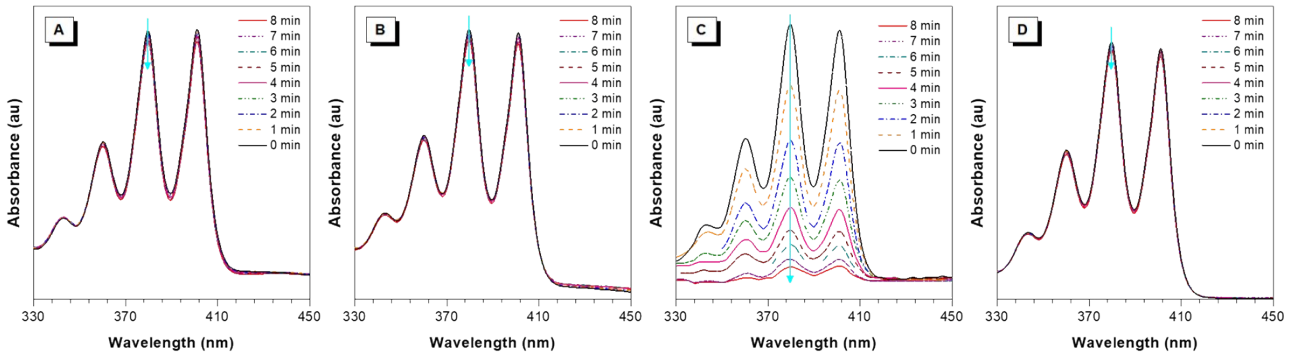

Figure S13. Absorption of ABDA in PBS in the presence of (A) *α*-TPA-PIO, (B) *β*-TPA-PIO, (C) MB or (D) pure DMSO after exposure to white light irradiation of 20 mW cm^{-2} with different time.

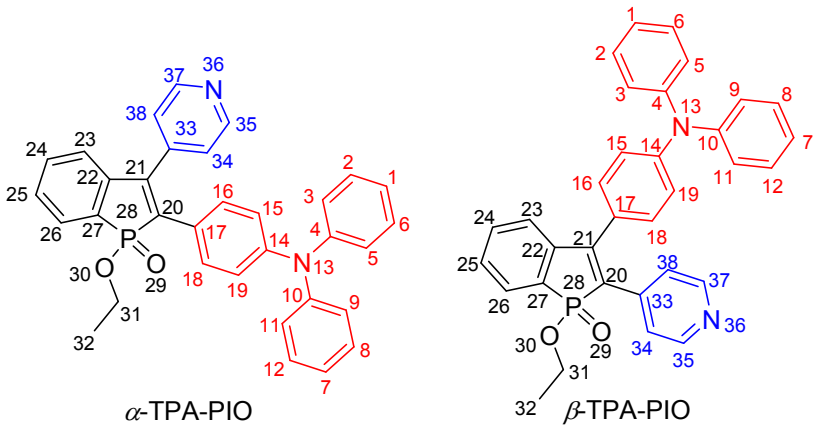

Figure S14. Atom numbers of *α*-TPA-PIO and *β*-TPA-PIO.

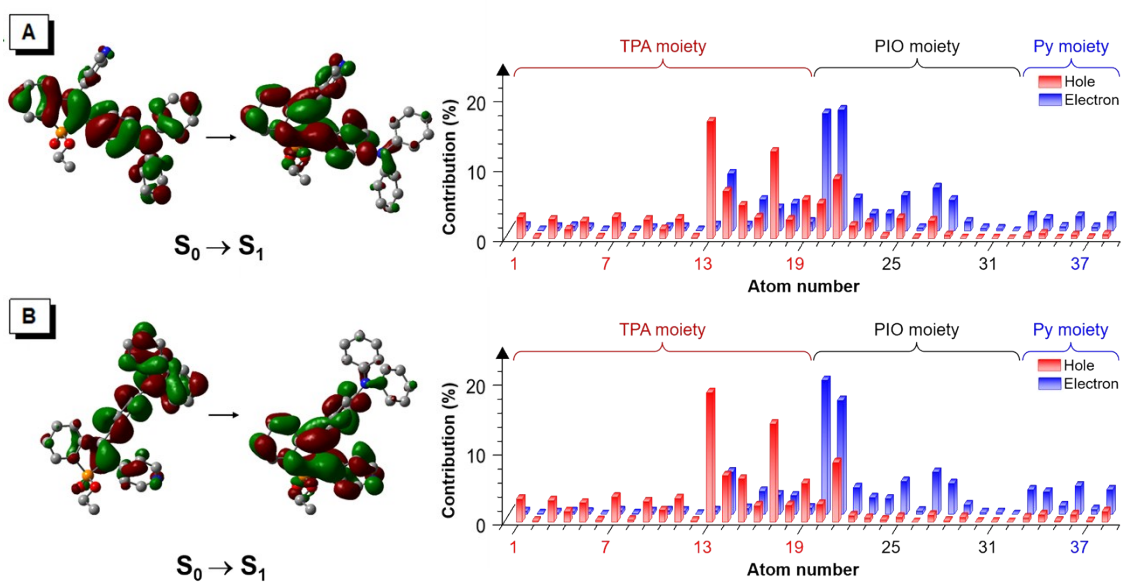

Figure S15. NTOs and atom contribution to hole and electron of the transition at the optimized S_0 state structures of (A) α-TPA-PIO and (B) β-TPA-PIO.

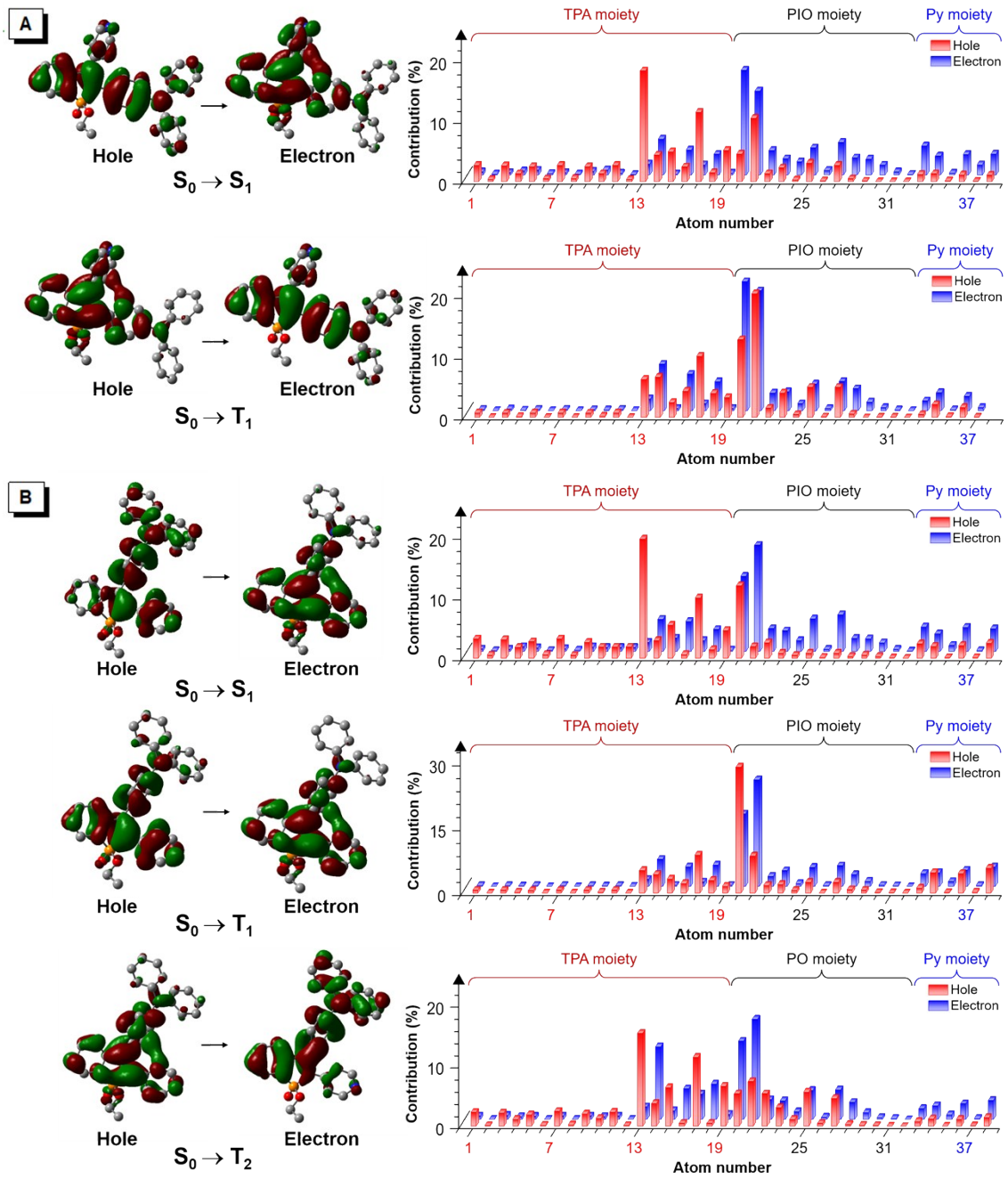

Figure S16. NTOs and atom contribution to hole and electron of the transition at the optimized S_1 state structures of (A) *α*-TPA-PIO and (B) *β*-TPA-PIO.

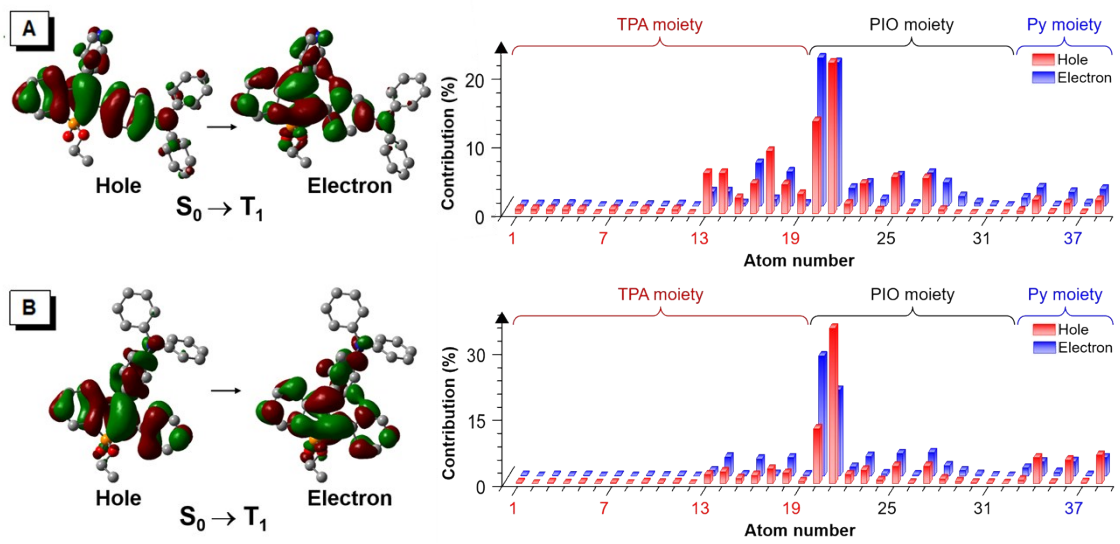

Figure S17. NTOs and atom contribution to hole and electron of the transition at the optimized T_1 state structures of (A) *α*-TPA-PIO and (B) *β*-TPA-PIO.

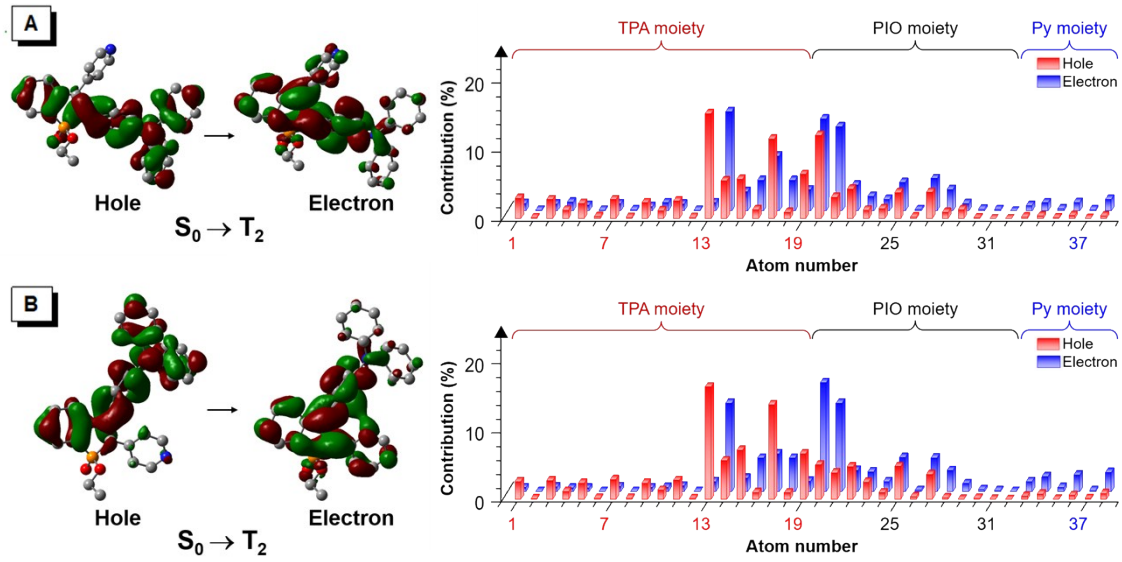

Figure S18. NTOs and atom contribution to hole and electron of the transition at the optimized T_2 state structures of (A) *α*-TPA-PIO and (B) *β*-TPA-PIO.

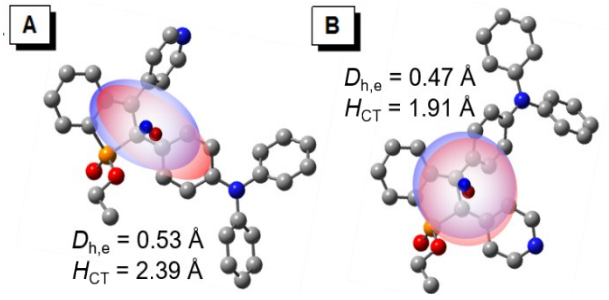

Figure S19. Centroids of hole (red region) and electron (blue region) of the $S_0 \rightarrow T_1$ transition of the optimized T_1 state structures of (A) *α*-TPA-PIO and (B) *β*-TPA-PIO, with labels of the centers of hole (red point) and electron (blue point) and $D_{h,e}$ and H_{CT}.

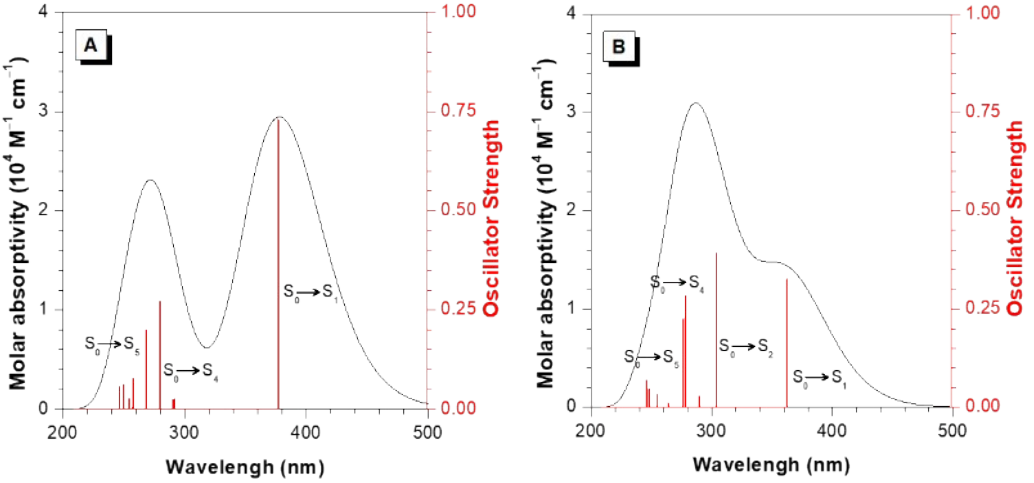

Figure S20. Calculated absorption spectra with oscillator strengths of (A) *α*-TPA-PIO and (B) *β*-TPA-PIO.

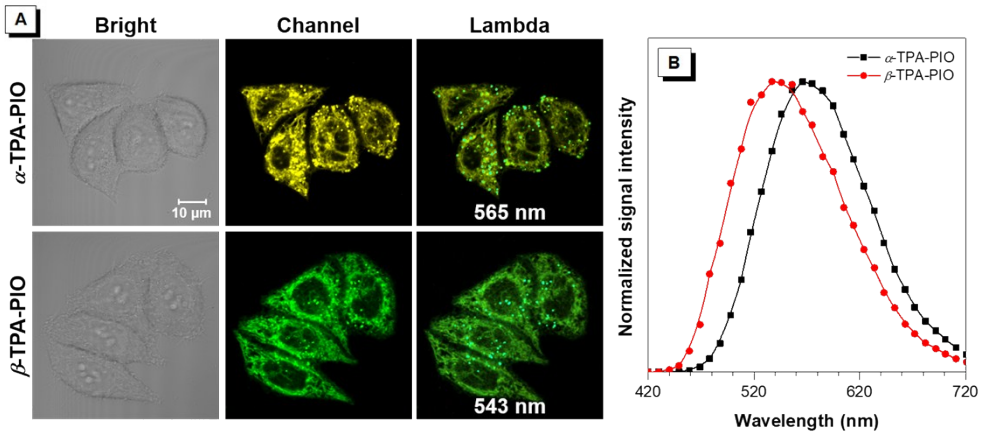

Figure S21. (A) Fluorescence channel and lambda stack images with bright-field of HeLa cells incubated with 1 μM *α*-TPA-PIO or *β*-TPA-PIO for 30 min using CLSM. (B) Normalized lambda spectra (plots of emission signal intensity *vs.* tacking wavelength) of *α*-TPA-PIO or *β*-TPA-PIO.

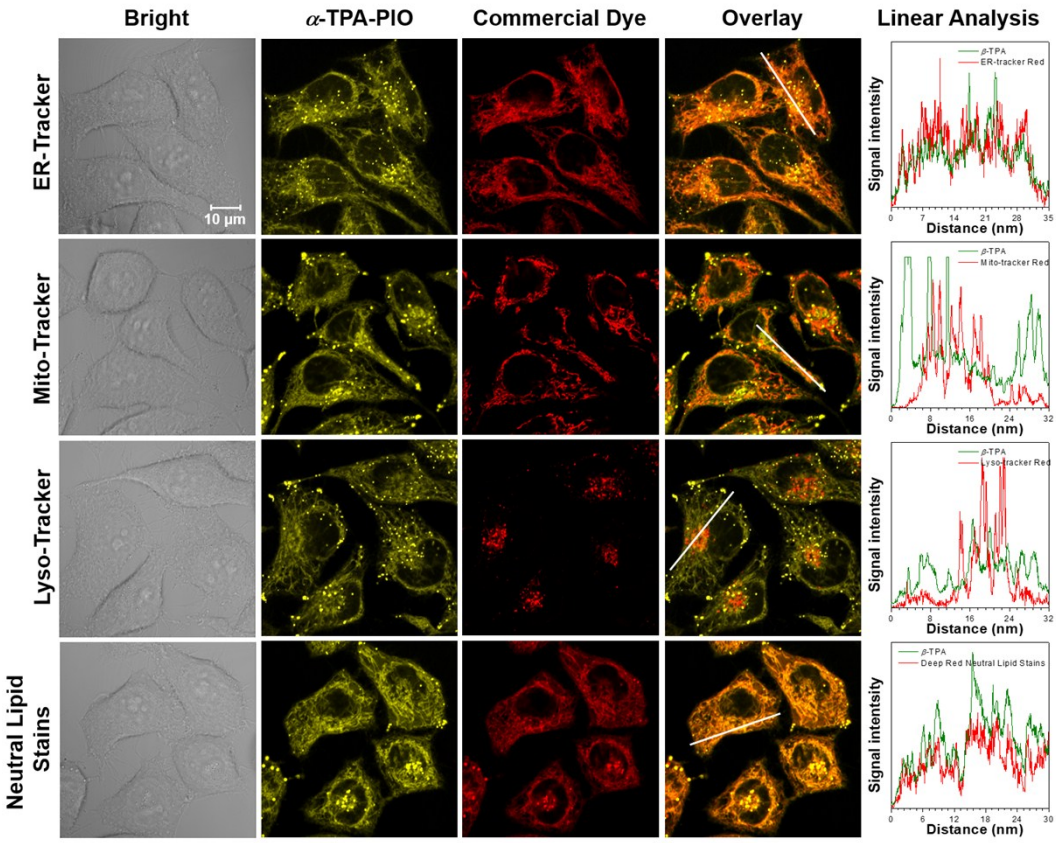

Figure S22. Colocalization images of HeLa cells co-stained with *α*-TPA-PIO and ER-Tracker Red, Mito-Tracker Red, Lyso-Tracker Red or HCS LipidTOX™ Deep Red neutral lipid stain, with the intensity profile of synchrony for the drew white line.

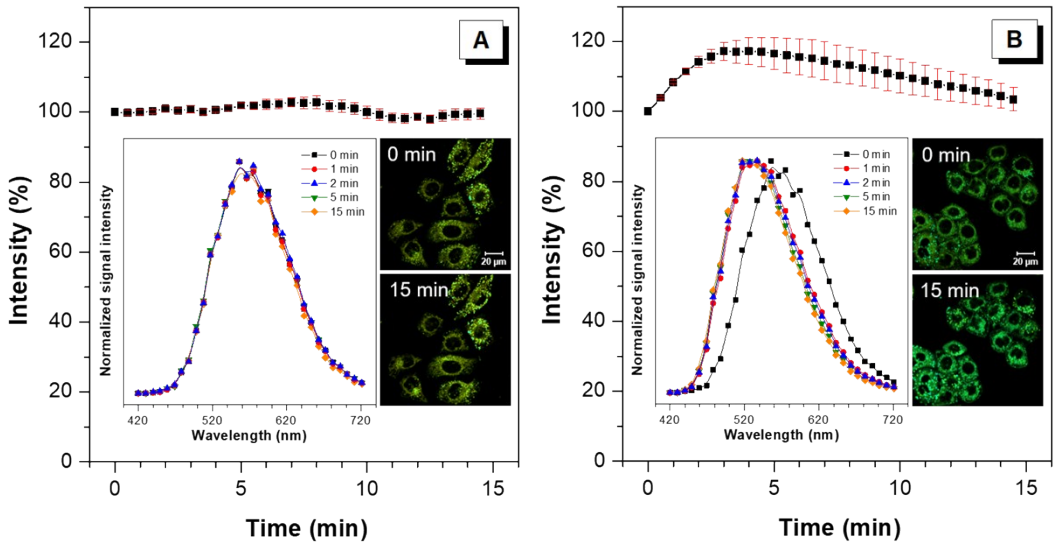

Figure S23. Photobleaching resistance assay of (A) *α*-TPA-PIO and (B) *β*-TPA-PIO in HeLa cells with continuous excitation and sequential scanning of irradiation using 405 nm laser of 10% power. Inset: Lambda stacking images and normalized lambda spectra at different time.

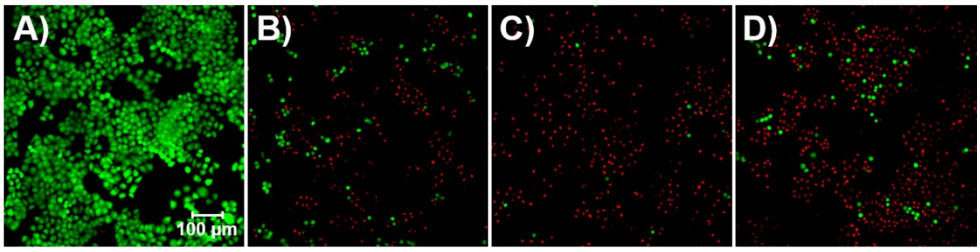

Figure S24. Live/dead cell co-staining assay by using calcein-AM with green fluorescence for live cells and PI with red fluorescence for dead cells: (A) the control group, (B) *α*-TPA-PIO and (C) *β*-TPA-PIO in normal condition and (D) *β*-TPA-PIO in hypoxic condition at the concentration of 10 μM, in presence of white light irradiation of 20 mW cm^{-2} for 30 min.

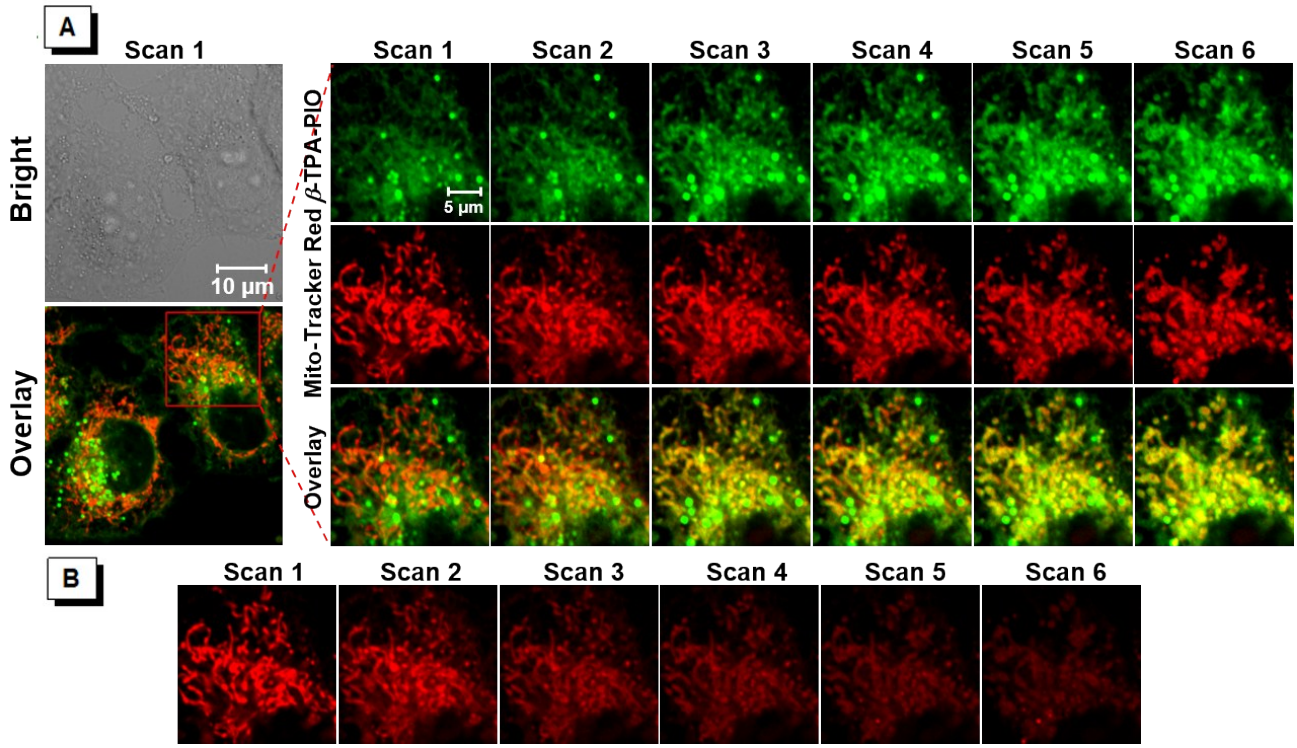

Figure S25. (A) Colocalization images of HeLa cells co-stained with *β*-TPA-PIO and Mito-Tracker Red (with brightness correction using ZEN 2012 (black edition)) with continuous irradiation of 405 nm laser of 1% power. (B) Original picture of the colocalization images of HeLa cells stained with Mito-Tracker Red without brightness correction. The signal intensity declines with continuous scanning for the poor photostability of Mito-Tracker Red.

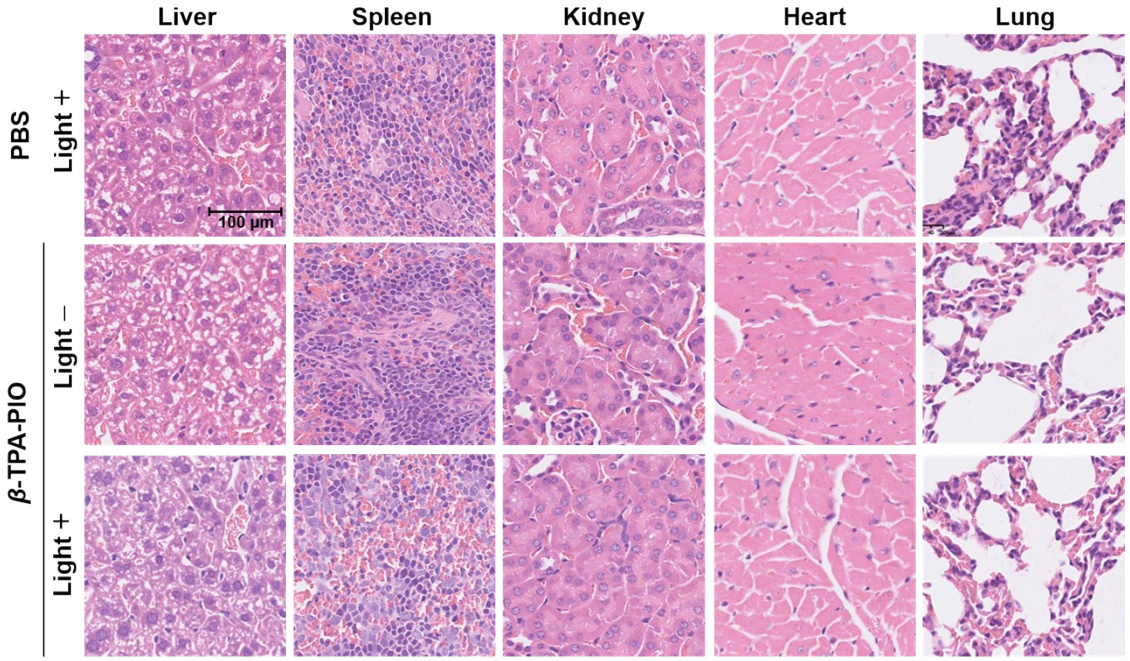

Figure S26. Histological H&E staining of various organ tissues in mice after different treatments.

Table S1. Photophysical properties of *α*-TPA-PIO and *β*-TPA-PIO in different states.

		α-TPA-PIO				*β*-TPA-PIO			
State	Δf [a]	λ_{abs} [b] (nm)	ε [c] (10^4 $M^{-1}cm^{-1}$)	λ_{em} [d] (nm)	Φ_F [e] (%)	λ_{abs} (nm)	ε (10^4 $M^{-1}cm^{-1}$)	λ_{em} (nm)	Φ_F (%)
Toluene	0.014	417	1.91	545	50.2	399	0.79	520	5.8
Butyl ether	0.096	412	1.92	534	44.7	392	0.72	511	5.5
Isopropyl ether	0.145	409	1.83	540	43.7	390	0.69	521	4.6
Ethyl ether	0.167	407	1.78	543	33.0	390	0.73	525	3.4
THF	0.210	411	1.76	563	44.6	393	0.76	560	12.2
Ethyl acetate	0.200	407	1.64	565	41.2	391	0.69	563	10.3
Isopropanol	0.273	420	1.39	598	17.2	410	0.66	598	3.1
Acetonitrile	0.305	407	1.67	602	15.3	394	0.71	613	3.7
DMF	0.276	411	1.72	600	18.7	409	0.69	611	5.0
DMSO	0.265	414	1.69	607	12.5	402	0.70	614	1.6
PBS[f]	/	430	1.76	576	44.8	408	0.98	563	8.6
Film[g]	/	/	/	573	33.7	/	/	560	15.3

[a] Orientation polarizability, $\Delta f = (\varepsilon - 1)/(2\varepsilon + 1) - (n^2 - 1)/(2n^2 + 1)$, where ε = dielectric constant and n = refractive index; [b] Absorption maximum measured in solution (10 μM); [c] Molar absorptivity; [d] Emission maxima measured in solution (10 μM) or film, excited at λ_{abs}; [e] Absolute fluorescence quantum yield determined using a calibrated integrating sphere; [f] With 1 *vol*% DMSO; [g] Drop-cast film on a quartz plate.

Table S2. Orthogonal coordinates for optimized S_0, S_1, T_1, and T_2 state structures of α-TPA-PIO.

	Opt (S_0)	Opt (S_1)	Opt (T_1)	Opt (T_2)
C1	5.6142, 3.6510, 0.4336	5.6541, 3.5663, 0.3696	4.8334, 3.5101, 3.9209	5.3252, 3.6318, 0.9396
C2	4.5493, 3.4994, –0.4504	4.6281, 3.4065, –0.5585	4.2338, 3.3818, 2.6693	4.2023, 3.5321, 0.1212
C3	3.9388, 2.2619, –0.6135	3.9643, 2.1923, –0.6694	3.6676, 2.1724, 2.2806	3.6749, 2.2900, -0.2011
C4	4.3801, 1.1613, 0.1258	4.3252, 1.1304, 0.1639	3.6857, 1.0855, 3.1598	4.2761, 1.1285, 0.3022
C5	5.4441, 1.3141, 1.0183	5.3558, 1.2838, 1.0938	4.2872, 1.2087, 4.4153	5.4037, 1.2258, 1.1283
C6	6.0593, 2.5518, 1.1625	6.0160, 2.5013, 1.1906	4.8611, 2.4192, 4.7882	5.9211, 2.4737, 1.4390
C7	6.1994, –3.5390, –0.2567	6.0063, –3.6081, 0.0760	5.3438, –3.6480, 3.5695	6.2604, –3.3842, –0.8592
C8	6.5528, –2.3784, –0.9390	6.3758, –2.5186, –0.7094	5.9572, –2.5435, 2.9800	6.5919, –2.1033, –1.3008
C9	5.7442, –1.2500, –0.8776	5.6002, –1.3676, –0.7231	5.2236, –1.3943, 2.7065	5.7648, –1.0267, –1.0209
C10	4.5733, –1.2673, –0.1150	4.4450, –1.3057, 0.0594	3.8658, –1.3473, 3.0326	4.5902, –1.2272, –0.2836
C11	4.2225, –2.4296, 0.5777	4.0754, –2.3905, 0.8580	3.2485, –2.4468, 3.6352	4.2555, –2.5119, 0.1636
C12	5.0290, –3.5581, 0.4969	4.8561, –3.5389, 0.8576	3.9893, –3.5956, 3.8934	5.0908, –3.5807, –0.1289
N13	3.7605, –0.1064, –0.0349	3.6540, –0.1213, 0.0558	3.1167, –0.1620, 2.7694	3.7278, –0.1389, –0.0094
C14	2.3579, –0.2097, –0.0819	2.2822, –0.1856, –0.0227	1.8780, –0.2257, 2.1595	2.3500, –0.3076, –0.0562
C15	1.5525, 0.6590, 0.6683	1.4714, 0.8430, 0.5186	0.9119, 0.7936, 2.3534	1.5029, 0.3989, 0.8526
C16	0.1731, 0.5625, 0.6147	0.1075, 0.7902, 0.4213	–0.3104, 0.7409, 1.7356	0.1445, 0.2469, 0.7899
C17	–0.4542, –0.4084, –0.1783	–0.5602, –0.3035, –0.2241	–0.6773, –0.3467, 0.8706	–0.4599, –0.5793, –0.2003
C18	0.3572, –1.2914, –0.9033	0.2802, –1.3436, –0.7419	0.3140, –1.3777, 0.7082	0.3877, 1.2951, –1.0902
C19	1.7385, –1.1877, –0.8694	1.6401, –1.2915, –0.6511	1.5341, –1.3212, 1.3191	1.7515, –1.1767, –1.0201
C20	–1.9157, –0.5426, –0.2344	–1.9652, –0.4187, –0.3176	–1.9187, –0.4670, 0.2326	–1.9115, –0.6795, –0.3053
C21	–2.8689, 0.4135, –0.1805	–2.9614, 0.5917, –0.0885	–2.9992, 0.5353, 0.1515	–2.8527, 0.3531, –0.2979
C22	–4.2746, –0.0867, –0.1782	–4.2886, 0.0572, 0.0936	–4.2744, –0.0389, –0.1797	–4.2341, –0.0992, –0.2233
C23	–5.4283, 0.6884, –0.1865	–5.4988, 0.7706, 0.2562	–5.5005, 0.6382, –0.3884	–5.4003, 0.6833, –0.3294
C24	–6.6717, 0.0538, –0.2264	–6.6955, 0.0868, 0.3627	–6.6300, –0.0756, –0.7475	–6.6403, 0.0677, –0.3430
C25	–6.7689, –1.3319, –0.2763	–6.7503, –1.3125, 0.2741	–6.5843, –1.4640, –0.9493	–6.7662, –1.3297, –0.2719
C26	–5.6118, –2.1152, –0.2880	–5.5823, –2.0332, 0.0504	–5.3759, –2.1428, –0.8107	–5.6238, –2.1240, –0.1955
C27	–4.3814, –1.4852, –0.2249	–4.3703, –1.3611, –0.0295	–4.2394, –1.4423, –0.4252	–4.3805, –1.5154, –0.1439
P28	–2.7145, –2.1739, –0.2732	–2.7567, –2.0247, –0.4348	–2.5527, –2.0503, –0.3043	–2.7479, –2.2619, –0.1027
O29	–2.4109, –3.1280, –1.3702	–2.6557, –2.8806, –1.6528	–2.0050, –2.7718, –1.4938	–2.4805, –3.3961, –1.0275
O30	–2.3646, –2.7143, 1.1995	–2.1668, –2.7820, 0.8725	–2.4426, –2.9417, 1.0511	–2.3978, –2.6020, 1.4370
C31	–2.9438, –3.9593, 1.6517	–2.5772, –4.1372, 1.1338	–2.9434, –4.2896, 1.0073	–3.0183, –3.7513, 2.0506
C32	–2.3514, –4.2748, 3.0032	–1.7619, –4.6492, 2.2975	–2.4562, –5.0077, 2.2455	–2.4322, –3.9095, 3.4326
C33	–2.5977, 1.8701, –0.1591	–2.6890, 2.0097, –0.2178	–2.7479, 1.9683, 0.1754	–2.4694, 1.7703, –0.3557
C34	–1.8736, 2.4758, –1.1848	–1.7996, 2.4886, –1.2022	–1.6095, 2.5097, –0.4519	–1.4617, 2.2097, –1.2254
C35	–1.6307, 3.8415, –1.1145	–1.5468, 3.8479, –1.2936	–1.3991, 3.8805, –0.4151	–1.1180, 3.5521, –1.2428
N36	–2.0501, 4.6174, –0.1123	–2.0829, 4.7679, –0.4854	–2.2091, 4.7476, 0.2048	–1.6852, 4.4780, –0.4613
C37	–2.7457, 4.0314, 0.8636	–2.9155, 4.3152, 0.4615	–3.2806, 4.2318, 0.8183	–2.6384, 4.0579, 0.3724
C38	–3.0498, 2.6752, 0.8859	–3.2490, 2.9827, 0.6347	–3.5934, 2.8790, 0.8345	–3.0616, 2.7377, 0.4644

Table S3. Orthogonal coordinates of heavy atoms for optimized S_0, S_1, T_1, and T_2 state structures of *β*-TPA-PIO.

	Opt (S_0)	Opt (S_1)	Opt (T_1)	Opt (T_2)
C1	–4.8187, 8.7939, 0.3005	–4.7860, 8.9038, –0.0752	–4.7147, 9.0528, –0.5814	–4.7005, 8.9867, 0.0975
C2	–4.9795, 7.7297, –0.5827	–4.9055, 7.8059, –0.9231	–4.8371, 7.8513, –1.2740	–4.9174, 7.8800, –0.7194
C3	–3.9592, 6.8043, –0.7645	–3.8944, 6.8565, –0.9882	–3.8429, 6.8844, –1.1899	–3.9426, 6.9009, –0.8486
C4	–2.7667, 6.9267, –0.0465	–2.7582, 7.0041, –0.1883	–2.7182, 7.1069, –0.3909	–2.7383, 7.0286, –0.1476
C5	–2.6072, 7.9903, 0.8450	–2.6295, 8.1075, 0.6589	–2.5960, 8.3104, 0.3080	–2.5149, 8.1399, 0.6733
C6	–3.6266, 8.9207, 1.0078	–3.6450, 9.0519, 0.7105	–3.5878, 9.2781, 0.2042	–3.4968, 9.1119, 0.7897
C7	2.2490, 7.3746, –0.5223	2.2486, 7.4103, –0.4447	2.3212, 7.3992, –0.4841	2.3023, 7.1186, –0.4920
C8	1.2167, 8.0467, –1.1705	1.2635, 7.9957, –1.2364	1.3773, 7.9225, –1.3632	1.3378, 7.8622, –1.1711
C9	–0.0907, 7.5839, –1.0842	–0.0469, 7.5419, –1.1769	0.0553, 7.4979, –1.3123	–0.0007, 7.5081, –1.1004
C10	–0.3823, 6.4442, –0.3298	–0.3738, 6.4922, –0.3150	–0.3368, 6.5494, –0.3649	–0.3811, 6.3969, –0.3388
C11	0.6526, 5.7750, 0.3301	0.6084, 5.9075, 0.4891	0.6066, 6.0312, 0.5253	0.5834, 5.6494, 0.3481
C12	1.9591, 6.2356, 0.2237	1.9160, 6.3673, 0.4161	1.9296, 6.4502, 0.4563	1.9193, 6.0140, 0.2649
N13	–1.7209, 5.9827, –0.2274	–1.7192, 6.0333, –0.2438	–1.6931, 6.1269, –0.3010	–1.7463, 6.0218, –0.2644
C14	–2.0065, 4.6051, –0.2664	–2.0102, 4.6880, –0.2266	–2.0134, 4.7700, –0.1730	–2.1015, 4.6850, –0.2888
C15	–3.0543, 4.0701, 0.4942	–3.1917, 4.2145, 0.4114	–3.1787, 4.3670, 0.5048	–3.2211, 4.2122, 0.4603
C16	–3.3307, 2.7118, 0.4513	–3.4792, 2.8777, 0.4420	–3.5106, 3.0332, 0.6123	–3.5225, 2.8766, 0.4829
C17	–2.5541, 1.8459, –0.3234	–2.6134, 1.9109, –0.1481	–2.6937, 2.0151, 0.0627	–2.7448, 1.9313, –0.2444
C18	–1.5107, 2.3833, –1.0827	–1.4163, 2.4050, –0.7581	–1.4919, 2.4383, –0.5604	–1.6616, 2.4212, –1.0297
C19	–1.2464, 3.7422, –1.0682	–1.1337, 3.7428, –0.8129	–1.1716, 3.7723, –0.6948	–1.3367, 3.7480, –1.0469
C20	–2.7879, 0.3876, –0.3010	–2.9017, 0.5099, –0.1338	–3.0271, 0.6205, 0.1250	–2.9577, 0.4925, –0.1365
C21	–1.8408, –0.5322, –0.0093	–1.8835, –0.4957, –0.0247	–1.9438, –0.4481, 0.1437	–1.9111, –0.4365, 0.0512
C22	–4.1251, –0.1820, –0.6473	–4.2352, –0.0473, –0.3602	–4.3220, 0.0252, –0.0134	–4.2428, –0.1047, –0.4412
C23	–5.2485, 0.5341, –1.0416	–5.4287, 0.6494, –0.6254	–5.5836, 0.6772, –0.0468	–5.4493, 0.5619, –0.7408
C24	–6.4159, –0.1597, –1.3676	–6.5938, –0.0496, –0.9007	–6.7402, –0.0512, –0.2375	–6.5755, –0.1758, –1.0601
C25	–6.4597, –1.5480, –1.3236	–6.6087, –1.4475, –0.9632	–6.7141, –1.4403, –0.4326	–6.5332, –1.5773, –1.1246
C26	–5.3254, –2.2744, –0.9515	–5.4272, –2.1525, –0.7687	–5.4906, –2.0984, –0.4740	–5.3358, –2.2526, –0.8728
C27	–4.1774, –1.5836, –0.6054	–4.2623, –1.4611, –0.4565	–4.3194, –1.3829, –0.2651	–4.2120, –1.5264, –0.5268
P28	–2.5420, –2.1959, –0.1453	–2.6005, –2.1158, –0.2932	–2.6468, –1.9980, –0.4544	–2.5239, –2.0879, –0.2362
O29	–1.9167, –3.1957, –1.0483	–2.1256, –3.0338, –1.3690	–2.2679, –2.5436, –1.7849	–1.9411, –2.9923, –1.2688
O30	–2.5994, –2.6399, 1.3990	–2.4648, –2.7921, 1.1735	–2.3194, –2.9947, 0.7663	–2.4768, –2.7488, 1.2421
C31	–3.2182, –3.9011, 1.7420	–2.9736, –4.1255, 1.3662	–2.8240, –4.3480, 0.7367	–2.9304, –4.1055, 1.4061
C32	–3.0815, –4.0921 3.2324	–2.6192, –4.5585, 2.7687	–2.0646, –5.1448, 1.7697	–2.6096, –4.5356, 2.8177
C33	–0.4536, –0.3157, 0.4334	–0.5655, –0.3619, 0.5004	–0.7090, –0.3698, 0.8365	–0.5801, –0.1982, 0.5607
C34	0.5635, –1.1707, 0.0010	0.4196, –1.3568, 0.2539	0.2975, –1.3462, 0.6263	0.4359, –1.1639, 0.3965
C35	1.8621, –0.9523, 0.4455	1.6956, –1.1997, 0.7492	1.5026, –1.2315, 1.2887	1.6932, –0.9447, 0.9313
N36	2.2048, 0.0298, 1.2794	2.1003, –0.1500, 1.4879	1.7887, –0.2468, 2.1543	2.0393, 0.1501, 1.6199
C37	1.2255, 0.8337, 1.7047	1.1733, 0.7732, 1.7545	0.8381, 0.6673, 2.3733	1.0769, 1.0643, 1.7890
C38	–0.1012, 0.7073, 1.3201	–0.1390, 0.7242, 1.3098	–0.4007, 0.6642, 1.7539	–0.2102, 0.9522, 1.2913

Table S4. Orthogonal coordinates of heavy atoms for optimized structures of α-TPA-PIO$^{\bullet-}$ and β-TPA-PIO$^{\bullet-}$.

α-TPA-PIO$^{\bullet-}$		β-TPA-PIO$^{\bullet-}$	
C1	5.6631, 3.6419, –0.3826	C1	–4.8913, 8.8888, –0.4226
C2	4.5147, 3.3503, –1.1132	C2	–4.9659, 7.6814, –1.1115
C3	3.8931, 2.1136, –0.9952	C3	–3.9242, 6.7644, –1.0489
C4	4.4083, 1.1426, –0.1271	C4	–2.7888, 7.0380, –0.2773
C5	5.5566, 1.4434, 0.6172	C5	–2.7200, 8.2479, 0.4236
C6	6.1780, 2.6780, 0.4801	C6	–3.7602, 9.1648, 0.3409
C7	5.9262, –3.6660, 0.6675	C7	2.2983, 7.3257, –0.0935
C8	4.6804, –3.4747, 1.2580	C8	1.3673, 8.0313, –0.8506
C9	3.9697, –2.2989, 1.0516	C9	0.0379, 7.6305, –0.8931
C10	4.4943, –1.2898, 0.2343	C10	–0.3878, 6.5178, –0.1579
C11	5.7425, –1.4903, –0.3698	C11	0.5490, 5.8123, 0.6070
C12	6.4502, –2.6640, –0.1450	C12	1.8790, 6.2126, 0.6296
N13	3.7625, –0.1046, 0.0082	N13	–1.7367, 6.0977, –0.1982
C14	2.3401, –0.1676, –0.0711	C14	–2.0389, 4.7085, –0.1775
C15	1.5459, 0.7014, 0.6794	C15	–3.0562, 4.2152, 0.6419
C16	0.1635, 0.6512, 0.5930	C16	–3.3464, 2.8575, 0.6613
C17	–0.4923, –0.2823, –0.2389	C17	–2.6221, 1.9419, –0.1187
C18	0.3326, –1.1645, –0.9716	C18	–1.5985, 2.4574, –0.9329
C19	1.7143, –1.1055, –0.8959	C19	–1.3176, 3.8129, –0.9731
C20	–1.9399, –0.3907, –0.3242	C20	–2.8875, 0.4982, –0.0818
C21	–2.9250, 0.5738, 0.0063	C21	–1.8699, –0.4903, –0.0284
C22	–4.2774, 0.0312, 0.0825	C22	–4.2175, –0.0344, –0.2992
C23	–5.4938, 0.7205, 0.2593	C23	–5.4202, 0.6762, –0.5001
C24	–6.6988, 0.0335, 0.2274	C24	–6.5971, –0.0058, –0.7652
C25	–6.7522, –1.3450, –0.0134	C25	–6.6284, –1.4035, –0.8736
C26	–5.5670, –2.0368, –0.2430	C26	–5.4453, –2.1215, –0.7211
C27	–4.3535, –1.3631, –0.1807	C27	–4.2660, –1.4513, –0.4234
P28	–2.7047, –1.9778, –0.5249	P28	–2.5989, –2.0952, –0.2690
O29	–2.5354, –2.8263, –1.7475	O29	–2.1405, –3.0575, –1.3210
O30	–2.2022, –2.8035, 0.7954	O30	–2.4713, –2.7822, 1.2091
C31	–2.6516, –4.1528, 0.9674	C31	–2.9881, –4.1067, 1.3859
C32	–1.9491, –4.7266, 2.1769	C32	–2.6419, –4.5608, 2.7854
C33	–2.6684, 2.0049, 0.0761	C33	–0.4991, –0.3647, 0.3913
C34	–1.7680, 2.6340, –0.8089	C34	0.4442, –1.3872, 0.1189
C35	–1.5432, 3.9954, –0.7158	C35	1.7507, –1.2677, 0.5503
N36	–2.1254, 4.7990, 0.1857	N36	2.2355, –0.2209, 1.2364
C37	–2.9711, 4.2057, 1.0361	C37	1.3472, 0.7441, 1.5092
C38	–3.2700, 2.8521, 1.0272	C38	0.0167, 0.7293, 1.1295

Table S5. Structure parameters of α-TPA-PIO, β-TPA-PIO and their radical anions α-TPA-PIO$^{\bullet-}$ and β-TPA-PIO$^{\bullet-}$.

		α-TPA	α-TPA$^{\bullet-}$	Δ^a			β-TPA	β-TPA$^{\bullet-}$	Δ^a
Bond Length (Å)	C17-C20	1.469	1.456	–0.013	**Bond Length (Å)**	C20-C33	1.472	1.439	–0.033
	C21-C33	1.482	1.454	–0.028		C17-C21	1.477	1.468	–0.009
	C20-C21	1.351	1.418	0.067		C20-C21	1.352	1.420	0.068
	C21-C22	1.492	1.459	–0.033		C21-C22	1.494	1.449	–0.045
	C22-C23	1.390	1.409	0.019		C22-C23	1.389	1.411	0.022
	C23-C24	1.397	1.387	–0.01		C23-C24	1.397	1.386	–0.011
	C24-C25	1.390	1.400	0.010		C24-C25	1.390	1.402	0.012
	C25-C26	1.397	1.391	–0.006		C25-C26	1.397	1.392	–0.005
	C26-C27	1.384	1.389	0.005		C26-C27	1.384	1.389	0.005
	C22-C27	1.403	1.421	0.018		C22-C27	1.403	1.423	0.020
	C27-P28	1.804	1.793	–0.011		C27-P28	1.806	1.794	–0.012
	P28- C20	1.817	1.773	–0.044		P28- C20	1.811	1.779	–0.032
	P28-O29	1.485	1.498	0.013		P28-O29	1.485	1.498	0.013
	P28-O30	1.607	1.636	0.029		P28-O30	1.608	1.635	0.027
	O30- C31	1.446	1.433	–0.013		O30-C31	1.446	1.433	–0.013
	C31-C32	1.509	1.512	0.003		C31-C32	1.509	1.511	0.002
Torsion Angle (°)	C16-C17-C20-C21	35.3	21.5	–13.8	**Torsion Angle (°)**	C38-C33-C20-C21	38.1	15.4	–22.7
	C17-C20-C21-C33	5.3	21.5	15.8		C33-C20-C21-C17	5.0	20.5	15.5
	C20-C21-C33-C34	57.7	35.5	–22.2		C20-C21-C17-C18	52.9	42.7	–10.2

[a] Δ = (α-TPA-PIO$^{\bullet-}$ – α-TPA-PIO) or (β-TPA-PIO$^{\bullet-}$ – β-TPA-PIO)

Table S6. Atomic charges with hydrogens summed into heavy atoms of α-TPA-PIO, β-TPA-PIO and their radical ions α-TPA-PIO$^{\bullet-}$ and β-TPA-PIO$^{\bullet-}$.

Atomic number	α-TPA-PIO	α-TPA-PIO$^{\bullet-}$	$\triangle^a$	Atomic number	β-TPA-PIO	β-TPA-PIO$^{\bullet-}$	$\triangle$
C1	–0.234	–0.311	–0.076	C1	–0.227	–0.139	0.088
C2	0.296	0.428	0.133	C2	0.211	0.126	–0.084
C3	–0.213	–0.328	–0.116	C3	–0.135	–0.117	0.018
C4	0.118	0.090	–0.027	C4	0.109	0.069	–0.040
C5	–0.168	–0.066	0.102	C5	–0.218	–0.100	0.119
C6	0.205	0.137	–0.068	C6	0.265	0.126	–0.139
C7	–0.236	–0.102	0.134	C7	–0.242	–0.169	0.073
C8	0.206	0.134	–0.072	C8	0.196	0.091	–0.105
C9	–0.179	–0.082	0.097	C9	–0.160	–0.060	0.100
C10	0.120	0.071	–0.049	C10	0.130	0.074	–0.055
C11	–0.193	–0.108	0.086	C11	–0.256	–0.173	0.083
C12	0.289	0.041	–0.248	C12	0.334	0.204	–0.130
N13	0.045	0.035	–0.010	N13	0.055	0.049	–0.006
C14	0.021	–0.047	–0.068	C14	0.103	0.114	0.011
C15	0.113	0.012	–0.101	C15	–0.017	–0.116	–0.098
C16	–0.122	0.055	0.178	C16	0.030	0.140	0.110
C17	0.137	–0.074	–0.210	C17	–0.172	–0.284	–0.112
C18	–0.241	–0.057	0.184	C18	0.178	0.250	0.072
C19	0.080	–0.002	–0.082	C19	–0.142	–0.215	–0.072
TPA: Sum (C1-C19)	**0.043**	**–0.174**	**–0.217**	**TPA: Sum (C1-C19)**	**0.042**	**–0.128**	**–0.170**
C20	–0.082	–0.163	–0.080	C20	0.065	0.015	–0.050
C21	0.010	–0.018	–0.028	C21	–0.112	–0.169	–0.057
C22	0.025	–0.056	–0.081	C22	0.049	–0.061	–0.109
C23	0.044	0.001	–0.043	C23	0.040	0.007	–0.033
C24	0.021	0.006	–0.015	C24	0.031	–0.020	–0.050
C25	–0.021	–0.102	–0.082	C25	–0.019	–0.079	–0.060
C26	0.085	0.055	–0.031	C26	0.077	0.046	–0.031
C27	–0.134	–0.158	–0.023	C27	–0.139	–0.157	–0.019
P28	0.554	0.510	–0.044	P28	0.549	0.510	–0.039
O29	–0.512	–0.557	–0.045	O29	–0.512	–0.556	–0.044
O30	–0.287	–0.298	–0.011	O30	–0.287	–0.296	–0.009
C31	0.182	0.150	–0.032	C31	0.182	0.149	–0.032
C32	0.049	0.026	–0.023	C32	0.050	0.027	–0.022
PIO: Sum (C20-C32)	**–0.066**	**–0.604**	**–0.538**	**PIO: Sum (C20-C32)**	**–0.028**	**–0.543**	**–0.515**
C33	–0.007	–0.269	–0.261	C33	0.123	0.004	–0.119
C34	0.034	0.336	0.302	C34	–0.097	–0.039	0.058
C35	0.151	–0.034	–0.184	C35	0.176	0.086	–0.091

N36	–0.363	–0.424	–0.060	N36	–0.357	–0.420	–0.062
C37	0.133	0.082	–0.050	C37	0.134	0.080	–0.054
C38	0.075	0.085	0.010	C38	0.007	0.002	–0.005
Py: Sum (C33-C38)	**0.023**	**–0.222**	**–0.245**	**Py: Sum (C33-C38)**	**–0.014**	**–0.287**	**–0.273**

[a] Δ = (α-TPA-PIO$^{\bullet-}$ – α-TPA-PIO) or (β-TPA-PIO$^{\bullet-}$ – β-TPA-PIO)

Table S7. Band density measured by ImageJ software.

Time (h)	0[a]	0.5[b]	1[c]	2[c]	3[c]	6[c]
GRP78	6	7	19	17	19	21
CHOP	10	10	31	32	35	32
BCl-2	25	20	4	3	5	7
Cleaved caspase-3	8	9	26	28	28	26
LC3B-I	20	9	5	6	5	6
LC3B-II	7	8	35	37	40	36
LC3B-II/ LC3B-I	0.35	0.89	7.00	6.17	8.00	6.00
GAPDH	31	32	31	31	31	31

[a] With treatment; [b] After treatment with β-TPA-PIO in dark for 30 min; [c] After treatment with β-TPA-PIO in dark for 30 min and subsequent irradiation with white light of 20 mW cm^{-2} for 30 min, then being cultured in dark.

4. Reference

1. J. Tydlitáta, S. Achelle, J. Rodríguez-López, O. Pytela, T. Mikýsek, N. Cabon, F. R. Guen, D. Miklík, Z. Růžičková and F. Bureš, *Dyes Pigm.*, 2017, **146**, 467–478.
2. F. Maurer and C. Carey, Real-Time Measurement of Intracellular O_2 in Mammalian Cells. BMG LABTECH: AN290. See https://www.bmglabtech.com.
3. M. J. Frisch, G. W. Trucks, H. B. Schlegel, G. E. Scuseria, M. A. Robb, J. R. Cheeseman, G. Scalmani, V. Barone, B. Mennucci, G. A. Petersson, H. Nakatsuji, M. Caricato, X. Li, H. P. Hratchian, A. F. Izmaylov, J. Bloino, G. Zheng, J. L. Sonnenberg, M. Hada, M. Ehara, K. Toyota, R. Fukuda, J. Hasegawa, M. Ishida, T. Nakajima, Y. Honda, O. Kitao, H. Nakai, T. Vreven, J. A. Montgomery, Jr., J. E. Peralta, F. Ogliaro, M. Bearpark, J. J. Heyd, E. Brothers, K. N. Kudin, V. N. Staroverov, T. Keith, R. Kobayashi, J. Normand, K. Raghavachari, A. Rendell, J. C. Burant, S. S. Iyengar, J. Tomasi, M. Cossi, N. Rega, J. M. Millam, M. Klene, J. E. Knox, J. B. Cross, V. Bakken, C. Adamo, J. Jaramillo, R. Gomperts, R. E. Stratmann, O. Yazyev, A. J. Austin, R. Cammi, C. Pomelli, J. W. Ochterski, R. L. Martin, K. Morokuma, V. G. Zakrzewski, G. A. Voth,

P. Salvador, J. J. Dannenberg, S. Dapprich, A. D. Daniels, O. Farkas, J. B. Foresman, J. V. Ortiz, J. Cioslowski and D. J. Fox, Gaussian, Inc., Wallingford CT, 2013.

4. K. Aidas, C. Angeli, K. L. Bak, V. Bakken, R. Bast, L. Boman, O. Christiansen, R. Cimiraglia, S. Coriani, P. Dahle, E. K. Dalskov, U. Ekström, T. Enevoldsen, J. J. Eriksen, P. Ettenhuber, B. Fernández, L. Ferrighi, H. Fliegl, L. Frediani, K. Hald, A. Halkier, C. Hättig, H. Heiberg, T. Helgaker, A. C. Hennum, H. Hettema, E. Hjertenæs, S. Høst, I.-M. Høyvik, M. F. Iozzi, B. Jansik, H. J. Aa. Jensen, D. Jonsson, P. Jørgensen, J. Kauczor, S. Kirpekar, T. Kjærgaard, W. Klopper, S. Knecht, R. Kobayashi, H. Koch, J. Kongsted, A. Krapp, K. Kristensen, A. Ligabue, O. B. Lutnæs, J. I. Melo, K. V. Mikkelsen, R. H. Myhre, C. Neiss, C. B. Nielsen, P. Norman, J. Olsen, J. M. H. Olsen, A. Osted, M. J. Packer, F. Pawlowski, T. B. Pedersen, P. F. Provasi, S. Reine, Z. Rinkevicius, T. A. Ruden, K. Ruud, V. Rybkin, P. Salek, C. C. M. Samson, A. Sánchez de Merás, T. Saue, S. P. A. Sauer, B. Schimmelpfennig, K. Sneskov, A. H. Steindal, K. O. Sylvester-Hvid, P. R. Taylor, A. M. Teale, E. I. Tellgren, D. P. Tew, A. J. Thorvaldsen, L. Thøgersen, O. Vahtras, M. A. Watson, D. J. D. Wilson, M. Ziolkowski and H. Ågren, *WIREs Comput. Mol. Sci.*, 2014, **4**, 269–284.
5. K. Liu, S, Zhou, J.-Y. Kim, K. Tillison, D. Majors, D. Rearick, J. H. Lee, R. F. Fernandez-Boyanapalli, K. Barricklow, M. S. Houston and C. M. Smas, *Am. J. Physiol-Endoc. M.*, 2009, **297**, E1395–E1413.